Journal of Medicinal Chemistry

pubs.acs.org/jmc

Drug Annotation

Discovery of JNJ-63576253: A Clinical Stage Androgen Receptor Antagonist for F877L Mutant and Wild-Type Castration-Resistant Prostate Cancer (mCRPC)

Zhuming Zhang,* Peter J. Connolly, Heng Keang Lim, Vineet Pande, Lieven Meerpoel, Christopher Teleha, Jonathan R. Branch, Janine Ondrus, Ian Hickson, Tammy Bush, Leopoldo Luistro, Kathryn Packman, James R. Bischoff, Salam Ibrahim, Christopher Parrett, Yolanda Chong, Marco M. Gottardis, and Gilles Bignan*

Cite This: *J. Med. Chem.* 2021, 64, 909–924

Read Online

ACCESS | Metrics & More | Article Recommendations | Supporting Information

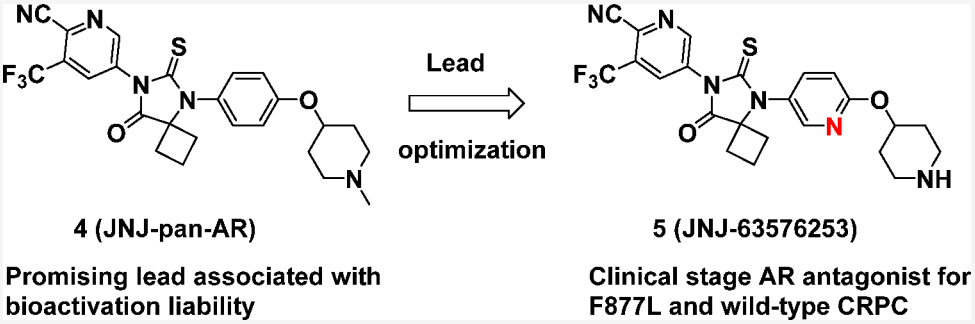

ABSTRACT: Persistent androgen receptor (AR) activation drives therapeutic resistance to second-generation AR pathway inhibitors and contributes to the progression of advanced prostate cancer. One resistance mechanism is point mutations in the ligand binding domain of AR that can transform antagonists into agonists. The AR F877L mutation, identified in patients treated with enzalutamide or apalutamide, confers resistance to both enzalutamide and apalutamide. Compound **4** (JNJ-pan-AR) was identified as a pan-AR antagonist with potent activity against wild-type and clinically relevant AR mutations including F877L. Metabolite identification studies revealed a latent bioactivation pathway associated with **4**. Subsequent lead optimization of **4** led to amelioration of this pathway and nomination of **5** (JNJ-63576253) as a clinical stage, next-generation AR antagonist for the treatment of castration-resistant prostate cancer (CRPC).

INTRODUCTION

Oncogenic activation of the androgen receptor (AR) is crucial for all stages of progressive prostate cancer.[1] Androgen deprivation therapy (ADT) such as abiraterone acetate effectively suppresses biosynthesis of endogenous androgens for AR activation.[2] AR-targeted antiandrogens such as enzalutamide (**1**, Figure 1) and apalutamide (**3**, ARN-509, Figure 2) block the binding of androgens to the androgen receptor.[3,4] Now approved by FDA as the standard of care for advanced prostate cancers, these second-generation AR antagonists show improved metastasis-free survival (MFS) for both castration-sensitive and castration-resistant prostate cancers.[5,4] However, as with other molecularly targeted cancer therapies in precision medicine, their efficacy is short-lived in many patients, and acquired resistance almost invariably emerges, resulting in disease progression to metastatic castration-resistant prostate cancer (mCRPC).[6] Genomic studies have established numerous resistance mechanisms such as gene alteration, amplification, and overexpression,[7,8] splice variant isoform expression (AR-V7),[9] ligand binding

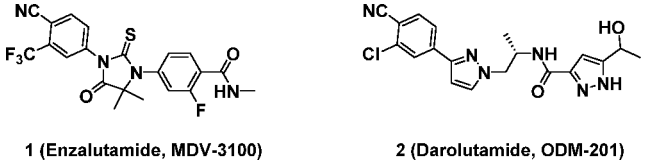

Figure 1. Chemical structures of enzalutamide, **1**, and darolutamide, **2**.

Received: September 7, 2020
Published: January 20, 2021

https://dx.doi.org/10.1021/acs.jmedchem.0c01563
J. Med. Chem. 2021, 64, 909–924

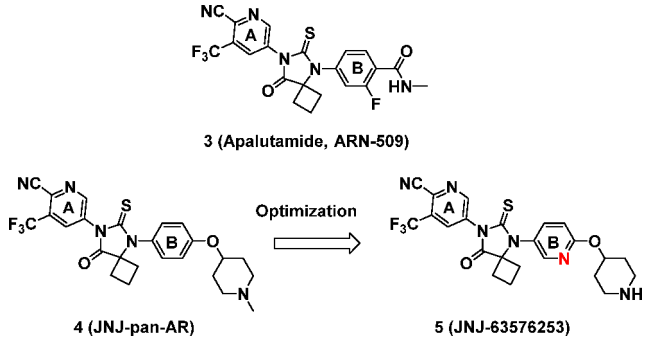

Figure 2. Chemical structures of **2** (Apalutamide ARN-509), **4** (JNJ-pan-AR), and **5** (JNJ-63576253). Ring "A" and Ring "B" (and its periphery) were the focus of our lead optimization efforts.

domain (LBD) point mutations,[10,11] and glucocorticoid receptor bypass.[12] Aberrant activation and persistent androgen receptor transcriptional signaling is now understood as the central core of resistant mechanisms in CRPC.[13] Continued reliance on AR provides a powerful rationale for retargeting the androgen/AR axis with next-generation AR pathway inhibitors.[14] Therefore, reactivation of AR signaling represents a major therapeutic opportunity as well as a challenge for treating mCRPC.[15]

Androgen receptor is a ligand-inducible transcription factor consisting of the N-terminal domain (NTD), DNA binding domain (DBD), and C-terminal ligand binding domain (LBD). To control the expression of AR regulated genes, the highly conserved DBD directly binds to DNA and thus allows constitutively active activation function 1 (AF1) in the NTD and ligand-dependent activation function 2 (AF2) in the LBD to stimulate transcriptional activities.[16]

Point mutations in the LBD of AR accounts for 10−20% of resistance and are characterized by receptor activation rather than inhibition upon ligand binding.[17] For example, four clinically relevant resistant mutations L702H, T878A, W742C, and W875L (formerly known as L701H, T877A, W741C, and W874L respectively) were identified for first-generation antiandrogens flutamide or bicalutamide.[18−21] Second-generation antiandrogens **1** and **3** were in part developed to overcome these resistance mechanisms.[3,4] In 2013, the mutation of phenylalanine to leucine at AR amino acid 877 (F877L, formerly known as F876L) was reported to confer resistance to both **1** and **3**, leading to antagonist-to-agonist switch in response to preclinical treatment *in vitro*.[10,11] In the clinic, AR F877L was detected in the plasma ctDNA for 3 of 29 progressing patients enrolled in the ARN-509 Phase I trial.[17] Recently, darolutamide (ODM-201, **2**, Figure 1) was reported to target resistance mechanisms including F877L mutation as a next-generation AR antagonist.[22]

In parallel to the development of **3**, we collaborated with Aragon Pharmaceuticals and screened a library of compounds to evaluate activity against wild-type AR as well as AR F877L and other clinically relevant mutants.[23] From this work, compound **4** (JNJ-pan-AR, Figure 2) was identified as a potential lead with favorable *in vitro* ADME and *in vivo* pharmacological properties. However, unacceptable toxicity findings hampered its further developability. We subsequently discovered an *in vitro* bioactivation pathway that could potentially explain the observed *in vivo* toxicity. Our hypothesis of blocking the bioactivation pathway served as the basis to initiate SAR studies for lead optimization. Here, we report our work on full characterization of **4** and additional studies leading to the selection of compound **5**, known as JNJ-63576253 (TRC-253) (Figure 2), highlighting data supporting its suitability for clinical development.

RESULTS AND DISCUSSION

In wild-type androgen receptor competitive radioligand binding assays (Table 1), **4** showed 2-fold better binding affinity (IC_{50} = 19 nM, K_i = 8.4 nM) than enzalutamide (**1**, IC_{50} = 38 nM, K_i = 17 nM) using labeled synthetic androgen R1881 (methyltrienolone) as the radioligand. Both compounds were highly selective over glucocorticoid receptor, GR (Table 1), and neither compound showed appreciable affinity for estrogen receptor, ER.

Table 1. Radioligand Binding of Compounds 4 and 1[a]

	4		1	
	IC_{50} (nM)	K_i (nM)	IC_{50} (nM)	K_i (nM)
AR	19	8.4	38	17
GR	20000	9900	29000	14000

[a]Radioligand binding inhibition and affinity calculations were determined using [^{3}H]methyltrienolone and [^{3}H]dexamethasone for AR and GR, respectively.

Having determined that **4** is a potent, competitive binder of AR, it was necessary to establish whether **4** acts as an antagonist or agonist.[10,24] The VP16 AR (WT and F877L) reporter system was chosen due to its highly sensitive response to ligand-dependent agonism (Supplementary Section S-2).[25] In these transcriptional reporter assays, we defined antagonism as the ability of a test compound to inhibit the response stimulated by low concentration of the synthetic androgen R-1881. Conversely, agonism was defined as the ability of a test compound to cause a response in the absence of exogenous androgen stimulation. In our hands, **4** completely inhibited signaling in HepG2 cells transiently transfected with VP16-AR F877L (IC_{50} = 127 nM) in the presence of R1881 (90 pM, antagonist mode), whereas in the same assay **1** only reached a maximal inhibition of 50% at any concentrations up to 30 μM (Table 6, Supplementary Figure S1a). When the VP16-AR F877L reporter assay was run in agonist mode (Supplementary Figure S1b), **1** elicited activation of the androgen receptor in the absence of R1881 in a dose-dependent manner starting at 1 nM, reaching 40% activity at 3 μM (Table 6, Supplementary Figure S1b). In contrast, **4** did not significantly activate AR and elicited only 10% maximal agonism at 300 nM in the absence of R1881. Because VP16-AR is constitutively nuclear and drives transcription through androgen response elements (AREs) in the absence of coactivator protein recruitment, this assay provides a direct assessment of ligand-induced DNA binding. We therefore conclude that **4** is effective in blocking ligand-induced DNA binding by AR.

To explore the activity of **4** in a native AR setting, ARE-luciferase reporter constructs were introduced into LNCaP prostate cancer cells, a model of prostate adenocarcinoma, that stably express either wild-type AR (LNCaP AR cs) or F877L mutant AR (LNCaP F877L).[26] Compound **4** was a full antagonist of the androgen-dependent reporter gene activity of both AR F877L and AR WT in the presence of R1881. As expected, enzalutamide (**1**) was an antagonist of AR WT. However, **1** was an incomplete antagonist in the presence of R1881 and behaved as an agonist in AR F877L cells at 10 μM

https://dx.doi.org/10.1021/acs.jmedchem.0c01563
J. Med. Chem. 2021, 64, 909−924

in the absence of R1881 (Table 2). To demonstrate that AR antagonism has an antiproliferative effect in androgen-dependent tumor cell lines, **4** and **1** were evaluated in the growth inhibition of VCaP cells (WT AR). Compound **4** inhibited the growth of VCaP cells with an IC_{50} of 92 nM, and the IC_{50} for **1** was 149 nM (Table 3 and Supplementary Figure S3). We thus conclude that **4** is equipotent to **1** in wild-type AR *in vitro*.

Table 2. Transcriptional Reporter Assay Activity of 1−18 in LNCaP F877L (Mutant) and LNCaP AR cs (WT) Cells

	LNCaP F877L		LNCaP WT	
compound	IC_{50} (nM)[b]	agonism[a]	IC_{50} (nM)[b]	agonism[a]
1	not fit	yes[c]	117 ± 66	no
4	98 ± 63	no	191 ± 120	no
5	37 ± 47	no	54 ± 53	no
7	85 ± 68	no	115 ± 89	no
8	145 ± 200	no	240 ± 580	no
9	427 ± 190	no	417 ± 64	no
10	309 ± 92[d]	no	501[e] ± 210	no
11	214 ± 92	no	302 ± 250	no
12	102 ± 110	no	162 ± 210	no
13	81 ± 43	no	120 ± 78	no
14	47 ± 27	no	50 ± 36	no
15	37 ± 16	no	76 ± 47	no
16	204 ± 150	no	355 ± 170	no
6	182 ± 45	no	204 ± 130	no
17	1000 ± 380	no	2239 ± 700	no

[a]LNCaP F877L and LNCaP WT reporter assays were repeated ≥3 times. Agonism is defined as complete, indicating activity was equal to that of R1881 stimulated reporter output. [b]Max inhibition >90% for all compounds except specifically mentioned. [c]Complete agonist at 10 μM. [d]Max inhibition 67%. [e]Max inhibition 85%.

Additionally, **4** was capable of effectively inhibiting transactivation of other clinically relevant AR ligand binding domain mutations, L702H, T878A, W742C, and W875L, in transiently transfected HepG2 cells (Supplementary Table S1).

Androgen receptor nuclear translocation occurs following ligand binding and intramolecular dimerization.[27] In an immunofluorescent imaging assay for AR protein localization (Supplementary Section S-5, Figure S2), **4** potently blocked nuclear translocation of AR F877L in both the presence and absence of R1881 in LNCaP F877L cells. Enzalutamide (**1**) partially inhibited nuclear translocation in the presence of R1881 and induced nuclear translocation of AR F877L to ∼50% of R1881-stimulated levels in the absence of R1881.[25] In contrast, both **4** and **1** inhibited androgen-stimulated nuclear translocation in wild-type LNCaP cells to a similar extent (Supplementary Figure S2). In this assay, **4** also inhibited the expression of PSA (KLK3), a protein whose expression is transcriptionally regulated by AR, in the presence of R1881 for both AR F877L and AR WT (data not shown).

The effect of **4** on androgen-dependent signaling was also assessed using the Hershberger assay as an *in vivo* PD model. In this assay, changes in weight of five androgen sensitive organs (ASOs) under stimulation by testosterone propionate (TP) were measured with or without AR antagonist treatment. Compound **4** was found to be a potent antagonist of ASO development *in vivo*, with activity equivalent to that of **1** when dosed at 30 mg/kg QD for 10 days (Supplementary Figure S4a).

Table 3. Antiproliferative Activity of 1, 4, 5, 7, 8, 11−16 in VCaP Prostate Cancer Cell Line[a]

compound	1	4	5	7	8	11	12	13	14	15	16
VCaP IC_{50} (nM)	149 ± 30	92 ± 71	265 ± 32	394 ± 431	306 ± 391	263 ± 224	277 ± 544	264 ± 39	250 ± 226	503 ± 647	2779 ± 1053

[a]VCaP cells (WT AR) were cultured in the presence of 30 pM R1881, and the extent of androgen-dependent proliferation was calculated. The VCaP antiproliferative assay was repeated ≥3 times.

https://dx.doi.org/10.1021/acs.jmedchem.0c01563
J. Med. Chem. 2021, 64, 909−924

To demonstrate *in vivo* activity in a prostate cancer model driven by AR F877L that is resistant to **1**, LNCaP F877L tumors were established in castrated SHO mice, and the antitumor activity of **4** was determined at 10 and 30 mg/kg orally once daily. At the end of study, tumor growth inhibition (TGI) was calculated using initial and final tumor volume measurements. TGIs of 80.2% and 100.8% (complete stasis) were obtained for the 10 mg/kg and 30 mg/kg cohorts respectively (Table 8 and Supplementary Figure S5a). Treatment with **4** led to complete stasis of tumor growth inhibition in a F877L-driven xenograft, whereas in a separate experiment no antitumor activity was observed in animals treated with **1** at 30 mg/kg orally once daily (Supplementary Section S-8).

To better understand the potential structural mechanism and binding mode of **1** in wild-type AR and AR F877L, we built a homology model representing a putative antagonistic AR conformation. It should be noted that to date no experimental structures of AR LBD in antagonist mode have been reported.[33] Our homology model of AR LBD was built using an antagonist-bound structure of glucocorticoid receptor as a template and used for various ligand docking calculations (Supplementary Section S-13).[29] The mechanism for antagonist-to-agonist switch could be rationalized by analogy, comparing the open and closed conformations, respectively, of Helix 12 located in LBD (Figure 3).[30,31] Enzalutamide (**1**)

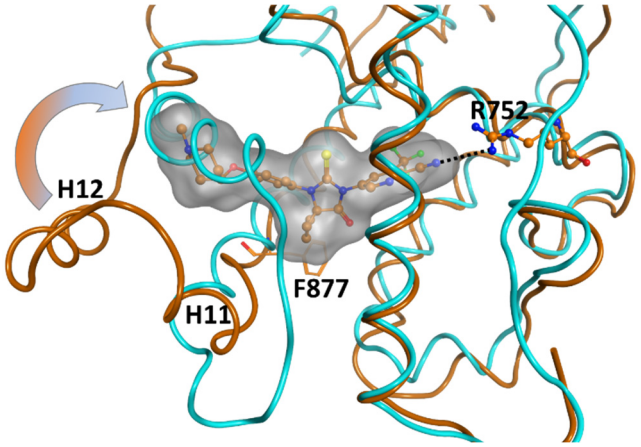

Figure 3. A manual docking model of **4** (orange balls and sticks with gray surface) with a potentially antagonistic conformation (orange tubes; homology model of AR built using GR PDB ID: 1NHZ) of AR LBD. Superposition of a crystal structure of AR in agonistic conformation (cyan tubes; PDB ID: 1T5Z) is shown as a reference to demonstrate the potential role of Helix 12 in modulating the pharmacology of AR.

was predicted to bind to the AR WT pocket in close proximity to Helix 12 and keep Helix 12 in an open, extended conformation described as the antagonist conformation.[32] Utilizing our molecular docking models, we hypothesized that the AR F877L mutation reduced steric hindrance in the ligand binding pocket and subsequently allowed **1** to freely rotate and point toward Helix 11 and the loop between Helices 11 and 12. The model suggested that this change potentially allowed Helix 12 to close, resulting in an agonistic conformation for **1**. Conversely, compound **4** was predicted to bind in close proximity to Helix 12 in an open conformation. Because of the presence of the bulky and charged piperidine group, **4** would have severe clashes with the protein in a putative agonistic conformation and should favor the antagonist conformation, resulting in functional antagonism of AR F877L and inactivation of transcription (Figure 3). This structural hypothesis would need additional experimental validation to broadly establish the idea that such a conformational switch is responsible for the observed pharmacological properties.

The attractive *in vitro* and *in vivo* pharmacological properties of **4** supported its further progression into single and repeat oral dose toleration 14-day studies in rats and dogs. Unfortunately, **4** displayed unacceptable hepatotoxicity in dogs, including liver necrosis, bile degeneration, and liver enzyme elevation (ALT, ALP, and GGT) at all doses (data not shown). Three major *in vivo* metabolites were detected in rat and dog plasma (respectively) by high resolution LC-MS on day 13: *N*-oxide M2 (2%, 20%), hydantoin M3 (2%, 0.2%), and *N*-des-methylpiperidine M4 (19%, 31%), consistent with findings from *in vitro* metabolite identification studies in human, rat, and dog hepatocytes. Significantly, a small amount of phenolic metabolite **6** (M1) was also observed *in vivo*, even though the percentage could not be estimated due to different ionization method utilized for identification by LC-MS (Figure 4).

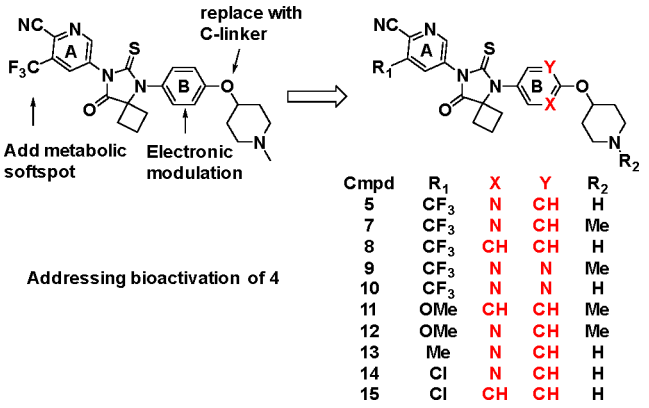

Cmpd	R_1	X	Y	R_2
5	CF_3	N	CH	H
7	CF_3	N	CH	Me
8	CF_3	CH	CH	H
9	CF_3	N	N	Me
10	CF_3	N	N	H
11	OMe	CH	CH	Me
12	OMe	N	CH	Me
13	Me	N	CH	H
14	Cl	N	CH	H
15	Cl	CH	CH	H

Figure 4. Proposed metabolic pathway of **4** in rat and dog plasma samples and potential bioactivation via M4 *in vivo*.

The detection of **6** (M1) *in vivo* raised the possibility of CYP450-mediated bioactivation of **4**. Phenolic structures are known to have safety liabilities; for example, it was reported that substituted phenols could act as uncouplers in mitochondrial oxidative phosphorylation.[28] In a GSH trapping experiment, an authentic sample of **6** formed glutathione adducts with a composition of M1+O+GSH-2H (2.1%) during incubation in dog liver microsomes in the presence of GSH and NADPH (Table 7). However, no GSH conjugate was detected from incubation of parent **4** in dog liver microsomes under the same conditions, suggesting the formation of **6** (M1) is a slow process due to low turnover of **4** *in vitro*. A putative bioactivation pathway was thus proposed involving the initial oxidative formation of *o*-quinone (M1+O) (Figure 4).

To determine whether reactive metabolites from phenol M4 were indeed responsible for observed hepatotoxicity (Figure 4), we began SAR studies to evade this bioactivation pathway and block the formation of a phenolic metabolite while simultaneously balancing the desirable *in vitro* and *in vivo* pharmacological parameters of **4**. Our systematic SAR analysis of the thiohydantoin chemotype suggested that keeping the basic piperidine nitrogen was favorable for full F877L

https://dx.doi.org/10.1021/acs.jmedchem.0c01563
J. Med. Chem. 2021, 64, 909−924

antagonism. Additionally, prior studies indicated that the middle thiohydantoin core, including the spiro-cyclobutyl feature, has been optimized.[23,34] Therefore, our next round of SAR iteration was focused on rational design of substituents on ring "A", ring "B", and its periphery by preserving the structural features of the key pharmacophore such as the critical cyano group (ring "A") that interacts with Arg752 via a hydrogen bond (Figure 3) and the pyridine nitrogen moiety (ring "A") for optimal potency and better plasma protein binding free fraction.

More than 200 analogues of **4** were synthesized with modifications on the ring "A" or "B" region.[35] Selected representatives are highlighted in Figure 5, including those

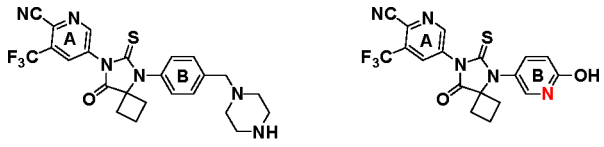

Figure 5. Chemical structures for close analogues of **4** designed to address bioactivation issues. The pyridone metabolite **17** of **5** is also shown.

with a metabolic soft spot remote from the bioactivation site (ring "A", **11**, **12**, and **13**), electronic alteration (ring "B", **5**, **7**, **9**, **10**, **12**, **13**, **14**), or a carbon-linker in place of oxygen (ring "B", **16**). Doubly modified compound **15** was chosen as a comparator to both **8** and **14**. Efforts to block or attenuate bioactivation by steric hindrance from additional substituents on ring "B" were also attempted but proved unsuccessful (data not shown).

The general syntheses of analogues and metabolites are outlined in Schemes 1–4.[35] In Scheme 1, cyano derivatives

Scheme 1. Synthesis of Thiohydantoin Analogues Metabolites or Intermediates 6, 17, and 22a–e[a]

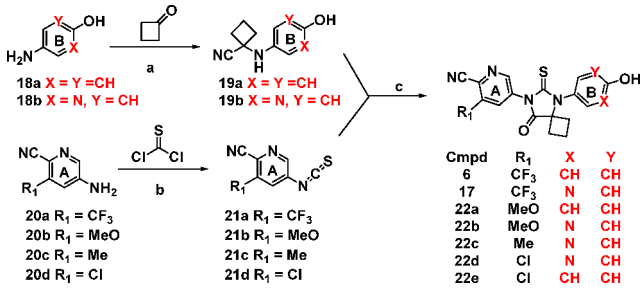

[a]Reagents and conditions: (a) TMSCN, ZnI_2 (cat), MeOH, rt or heating; (b) $CHCl_3/H_2O$/DMA, rt; (c) DMA, 60 °C.

19a–b were prepared via a Strecker reaction by heating commercially available or synthetically accessible amines **18a–b** in methanol or neat with cyclobutanone in the presence of trimethylsilyl cyanide and a catalytic amount of zinc iodide. Cyano derivatives **19a–b** were then cyclized to **6**, **17**, and **22a–e** in a one-pot reaction in dimethylacetamide by heating with isothiocyanates **21a–d**, freshly prepared from the corresponding anilines **20a–d**, followed by treatment with aqueous HCl solution.

In Scheme 2, the Mitsunobu reaction of **6**, **22a–b** with commercially available **23**, followed by treatment with HCl

Scheme 2. Synthesis of Thiohydantoin Analogues 4, 5, 7, 8, 13, 14, and 15[a]

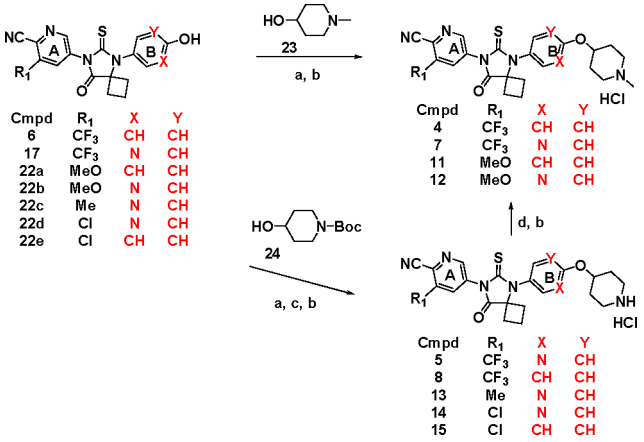

[a]Reagents and conditions: (a) DIAD or DEAD, PPh_3, THF, 60 °C; (b) HCl, 1,4-dioxane; (c) TFA; (d) HCHO, $NaBH(OAc)_3$.

provided corresponding analogues **4**, **11**, and **12** as HCl salts. Similarly, the Mitsunobu reaction of **6**, **17**, **22c–e** with commercially available **24**, followed by deprotection reaction and treatment with HCl, provided analogues **8**, **5**, **13–15**, respectively. Reductive amination of **5** with formaldehyde and sodium triacetoxyborohydride led to the formation of **7**.

Compounds **9** and **10** were prepared according to Scheme 3. Cyano derivative **19c** was prepared via a Strecker reaction by

Scheme 3. Synthesis of Thiohydantoin Analogues 9 and 10[a]

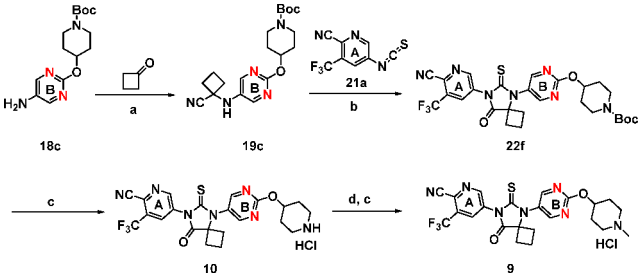

[a]Reagents and Cconditions: (a) NaCN, AcOH; (b) DMA, 60 °C; (c) HCl, 1,4-dioxane; (d) HCHO, $NaBH(OAc)_3$.

heating commercially available amine **18c** in acetic acid with cyclobutanone in the presence of sodium cyanide. **19c** was then cyclized to **22f** by heating with freshly prepared isothiocyanate **21a**, in dimethylacetamide. Treatment with anhydrous HCl in 1,4-dioxane solution provided **10** as HCl salt. Reductive amination of **10** with formaldehyde and sodium triacetoxyborohydride, followed by treatment of anhydrous HCl, afforded **9**. A variation of synthetic route Scheme 3, replacing **18c** with commercially available **18d**, afforded analogue **16** as shown in Scheme 4.

The synthesized analogues and selected metabolites (intermediates **6** and **17**) were evaluated in LNCaP AR F877L and LNCaP AR WT cellular reporter assays for luciferase transcriptional activities. The results are summarized in Table 2. Analogues **5**, **7–16**, and phenolic metabolites **6** and **17** all acted as full antagonists and inhibited luciferase transcription with IC_{50} values ranging from 30 to >2000 nM (Table 2). No agonism of either AR F877L or AR WT was observed for these compounds under the assay conditions.

https://dx.doi.org/10.1021/acs.jmedchem.0c01563
J. Med. Chem. 2021, 64, 909–924

Scheme 4. Synthesis of Thiohydantoin Analogue 16[a]

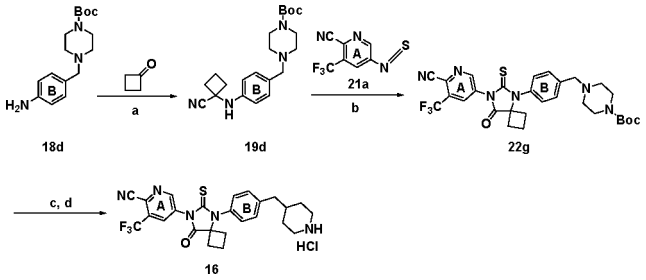

[a]Reagents and conditions: (a) NaCN, AcOH; (b) DMA, 60 °C; (c) TFA; (d) HCl, 1,4-dioxane.

Interestingly, analogue **8** (F877L IC_{50} = 145 nM; WT IC_{50} = 240 nM) was equally potent to *N*-methyl parent **4** (F877L IC_{50} = 98 nM; WT IC_{50} = 191 nM, Table 2). The potency of desmethyl **5** (F877L IC_{50} = 37 nM; WT IC_{50} = 54 nM) was 2-fold better compared to that of **7** (F877L IC_{50} = 85 nM; WT IC_{50} = 115 nM), confirming that piperidine without methyl substitution still maintained potency. Furthermore, both **5** and **7** were comparable or slightly more potent than **4** and **8**, indicating a pyridinyl "B" ring is well tolerated. In contrast, the pyrimidinyl "B" ring in **9** (F877L IC_{50} = 427 nM; WT IC_{50} = 417 nM) and **10** (F877L IC_{50} = 309 nM; WT IC_{50} = 501 nM) was less tolerated, evidenced by the loss of more than 3-fold potency. Methoxy (ring "A") modification (**11**, F877L IC_{50} = 214 nM; WT IC_{50} = 302 nM) lost 2-fold in potency, but potency was restored in combination with a pyridinyl "B" ring (**12**, F877L IC_{50} = 102 nM; WT IC_{50} = 162 nM). Similarly, methyl or chloro-modification in ring "A" in combination with pyridinyl (**13**, **14**) maintained good potency, similar to counterpart **15**. C-linker modification (**16**) reduced potency in both AR F877L mutant and AR WT (F877L IC_{50} = 204 nM; WT IC_{50} = 355 nM) compared to **4** or **8**. In contrast to phenol **6**, pyridone metabolite **17** lost 5- or 10-fold potency (F877L IC_{50} = 1000 nM; WT IC_{50} = 2239 nM) in relation to its corresponding parent **5** (or **7**).

To correlate AR antagonism with the antiproliferative effect in androgen-dependent tumor cell lines, **5**, **7**, **8**, and **11**–**16** were also evaluated in the growth inhibition of AR WT-dependent VCaP cells. Inhibition of luciferase transcription appeared to translate into antiproliferative activities in VCaP cells, tracking with LNCaP WT potency with IC_{50} values ranging from 250 to >2700 nM (Table 3). Despite comparable or better potency in LNCaP reporter assays, demethylated **8** (VCaP IC_{50} = 306 nM) was less potent compared to corresponding **4** (VCaP IC_{50} = 92 nM). Pyridone metabolite **16** is the least potent compound (VCaP IC_{50} = 1692 nM).

In mouse single-dose PK studies, **8**, the major active metabolite M4 of **4** (Figure 2) displayed comparable AUC (10.4 μg·h/mL) and C_{max} (1.17 μM) to that of **4** (AUC 9.4 μg·h/mL, C_{max} 0.98 μM) after oral dosing, with a shorter but still reasonable half-life ($T_{1/2}$10.5 h) compared to that of **4** ($T_{1/2}$46.4 h) in IV dosing (Table 4). The same trend was observed by comparing **5** and **7** in terms of exposure and half-life, indicating demethylated analogues still maintained the desirable PK characteristics of their parents. Furthermore, both **8** (HLM $T_{1/2}$ > 180 min) and **5** (HLM $T_{1/2}$ > 180 min) are more stable in human liver microsomes compared to **4** (HLM $T_{1/2}$ = 93.1 min) and **7** (HLM $T_{1/2}$ = 173 min). All analogues displayed favorable PK parameters with oral bioavailabilities ranging from 45% to >100% (Table 4)

All analogues except for **7** were tested in the Hershberger assay for their inhibitory effect on the five androgen sensitive organs (ASOs) under stimulation by testosterone propionate (TP). The pharmacodynamic (PD) results are summarized in Table 5. Because *in vivo* metabolite studies indicated that **5** was the major circulating, stable metabolite of **7** in mouse plasma, accumulating significantly in repeat-dosing PK studies, compound **5** was selected to be included for PD studies in the Hershberger assay. Compounds **5**, **8**, **11**, **12**, **14**, and **15** showed significant efficacy with 30 mg/kg once daily oral dosing (Table 5), comparable to that of control group flutamide with 10 mg/kg once daily oral dosing.

Table 5. PD Effect of 5, 8, 11–16 in Hershberger Assay on ASO (Seminal Vesicles and Prostate): QD × 10 Days Dosing

compound	5	8	11	12	13	14	15	16
PO dose (mg/kg)	30	10	30	30	30	30	30	30
ASO inhibition	yes	yes	yes	yes	no	yes	yes	no

Compounds **13** and **16** displayed no statically significant inhibitory effect in the Hershberger assay. Introduction of a metabolic soft spot in **13** and weaker *in vitro* potency in **16** (LNCaP WT IC_{50} 350 nM; VCaP IC_{50} 2779 nM) may contribute to the loss of *in vivo* efficacy. Nevertheless, the lack

Table 4. Human Liver Microsomal $T_{1/2}$, Permeability, and Mean Single Dose PK Parameters of Compound 4, 5, 7, 8, 11–16 in CD-1 Male Mice by PO and IV Dosing

compound	4	5	7	8	11	12	13	14	15	16
HLM_$T_{1/2}$ (min)[a]	93.1	>180	173	>180	114	135	>180	>180	>180	>180
P_{app} A > B (+inh.) (cm/s × 10^{-6})[c]	23.5	5.62	16.2	6.8	–	22.1	3.38	11.5	12.2	6.31
PO dose (mg/kg)	10	10	10	10	10	10	10	10	10	10
AUC_{last} (μg·h/mL)	9.4	4.9	10.9	10.4	20.1	6.1	7.8	6.0	4.6	8.7
C_{max} (μM)	0.98	0.66	1.3	1.17	2.8	1.32	1.88	1.88	0.78	0.84
IV dose (mg/kg)	2	2	2	2	2	2	2	2	2	2
CL (mL/min/kg)	4.12	15.0	8.14	8.3	6.9	8.8	19.4	25.4	26.7	18.2
$T_{1/2}$ (h)	46.4	5.99	12.5	10.5	7.8	4.2	3	4.1	3.7	12.1
Vdss (L/kg)	12.0	6.11	7.69	5.56	3.7	2.93	4.35	6.92	8.47	16.8
F (%)[b]	56	45	56	49	87	116	92	118	50	97

[a]For HLM $T_{1/2}$: High stability >180 min; 33 min < medium stability <180 min; low stability <33 min. [b]Oral bioavailability. [c]Passive permeability was measured from the apical (A) to the basolateral side (B) of the MDCK-MDR1 cells in the presence of a P-gp inhibitor with mass balance >60%.

https://dx.doi.org/10.1021/acs.jmedchem.0c01563
J. Med. Chem. 2021, 64, 909–924

Table 6. Summary of Maximal Inhibition (Antagonist Activity), EC_{50} and Maximal Stimulation (Agonist Activity) for 1, 4, 5, 8, 11−15 in VP16-AR F877L Mutant and VP16-AR WT HepG2 Reporter Assays[a]

	VP16-AR F877L			VP16-AR WT		
compound	% Inh_{max}	% E_{max}	EC_{50} (nM)[b]	% Inh_{max}	% E_{max}	EC_{50} (nM)[b]
1	86	40	61.8 ± 65.1	100	<5	NA
4	100	10	NA	100	<5	NA
5	100	10	NA	100	<5	NA
8	100	10	NA	100	<5	NA
11	100	35	649 ± 310	100	<5	NA
12	86	40	838 ± 527	>90	<5	NA
13	100	<5	NA	100	<5	NA
14	100	31	NA	100	<5	NA
15	>90	34	45 ± 20	100	<5	NA

[a]Agonist (EC_{50}) values for each of the AR cDNA used in the reporter assays are summarized. VP16-AR F877L and VP16-AR WT reporter assays were repeated ≥3 times, and similar results were obtained. Each compound was tested in concentrations ranging from 1 nM to 30 μM with a dilution factor 12. [b]All values are calculated relative to the activity of R1881-induced androgen receptor activity ($n \geq 3$) for indicated maximal inhibition or stimulation of induction of androgen dependent signaling (%).

Table 7. Incubation of 8, 6, 5, 17 in Dog Liver Microsomes with GSH in the Absence or Presence of NADPH[a]

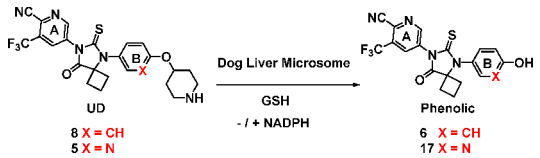

compound	**8**		**6**		**5**		**17**	
NADPH[b]	−	+	−	+	−	+	−	+
UD[c]	100%	99.8%	100%	91.9%	100%	98.8%	100%	100%
UD+O	−	0.01%	−	6.1%	−	0.6%	−	0.02%
UD+O+GSH-2	−	−	−	2.1%	−	−	−	−
phenolic (**6** or **17**)[d]	−	0.2%	NA	NA	−	0.6%	NA	NA

[a]Final concentrations of the substrates (UD), dog liver microsomes, glutathione (GSH), and NADPH were 10 μM, 1 mg/mL, 5 mM, and 1 mM, respectively. The percent compositions of parent drug and its metabolites were based on peak areas from 5 ppm accurate mass measurements and with assumptions of equal positive electrospray ionizations. [b]∓ means absence or in the presence of NADPH. [c]UD is defined as incubated substrate unchanged. [d]Phenolic refers to either metabolite **6** or **17**.

of *in vivo* activity for **13** was unexpected given its *in vitro* potency in VCaP (Table 3) and *in vivo* PK parameters (Table 4), which are comparable to those of **5**, **11**, and **14**.

In a follow-up studies, **11**, **12**, **14**, and **15** showed signs of partial agonism ranging from 30% to 43% maximal stimulation in the absence of R1881 in HepG2 cells transiently transfected with VP16-AR F877L, while **5**, **8**, and **13** exhibited no signs of agonism (<10%) in both AR F877L and AR WT cells (Table 6). The results were not in total agreement with those from natively stable AR LNCaP reporter assays. In particular, the phenotype of **11** and **12** strikingly resembles **1** (Table 6). Compound **12** is an incomplete antagonist and partial agonist in the VP16-AR F877L reporter assay. As noted previously, the VP16-AR reporter system is a highly sensitive assay for determining antagonism and agonism of the androgen receptor. This fusion protein elicits as much as a 20-fold stronger transcriptional activity than the natural AR but still reflects the intrinsic propensity of antagonism or agonism. These data were surprising because, compared to the CF_3 or Me group in **4**, **5**, **8**, and **13**, the MeO or Cl moiety in ring "A" of **11**, **12**, or **14** was considered to represent a minor change in terms of binding to the hydrophobic area of the LBD pocket in our homology model. The results indicate that there is still a lack of molecular understanding as to how exactly Helix 12 regulates the antagonist−agonist switch—for example, how Helix 12 affects coactivator binding to the leucine rich LxxLL motifs on AF2 induced after antagonist or agonist binding in LBD. Nevertheless, taken together, our results suggest that the CF_3 moiety on ring "A" has been optimized.

The chemical structures of **5** and **8** are similar except for a critical bioisosteric N/CH exchange in ring "B" (Figure 5). Both compounds share the identical ring "A" and hydantoin core, as well as the same peripheral piperidin-4-yloxy decoration. Their overall *in vitro* and *in vivo* profiles also track well and mirror each other (Tables 2−6). In fact, **5** and **8** were both first identified from metabolite studies of **4** and **7** respectively. The difference lies in the reactivity of key metabolites. Specifically, phenol **6**, the common metabolite from both **4** and **8**, can be bioactivated as indicated by the formation of a GSH adduct (2.1% UD+O+GSH-2H, Table 7), whereas pyridone **17**, the corresponding metabolite from **5**, is negative in the same GSH trapping experiments, as summarized in Table 7. Like **6**, pyridone **17** was also produced in only trace amounts (0.6%) presumably due to the low turnover of **5** under the *in vitro* assay conditions.

To demonstrate that improved safety did not come at the expense of *in vivo* efficacy, **5** was further evaluated in the prostate LNCaP SR*α* F877L tumor xenograft model driven by AR F877L in castrated SHO mice. In this model, **5** showed statistically significant tumor growth inhibition at 30 mg/kg, while **1** was not effective at 30 mg/kg QD compared to vehicle control (Figure 6). The antitumor activity of **5** was determined

https://dx.doi.org/10.1021/acs.jmedchem.0c01563
J. Med. Chem. 2021, 64, 909−924

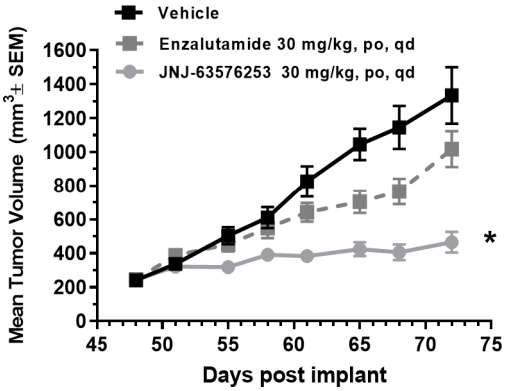

Figure 6. Oral *in vivo* efficacy profile of **5** (JNJ-63756253) in castrated male SHO mice implanted with LNCaP F877L tumors cells. Tumors were measured twice weekly, and the results presented as the average tumor volume, expressed in mm^3 ± SEM of each group. *Tumor growth inhibition (TGI) was statistically significant ($p < 0.05$) using a one-way ANOVA with multiple comparisons Dunnett's multiple comparisons post-test using Graph Pad Prism software (version 6).

at 30 mg/kg QD comparable to that of **4** as shown in Table 8. Taken together, our results support the continued development and advancement of **5** into human clinical trials.[35,36]

Table 8. *In vivo* Efficacy Data for 5 compared to 4 Based on the LNCaP F877L Tumor Xenograft Model

compound	4	5
dose (mg/kg)	30	30
tumor growth inhib. (%)	100.8	87
plasma exposure (ng/mL)	748	1750

Both **8** and **5** were advanced into single and repeat dose 14-day toleration studies. Compound **8** displayed unacceptable hepatotoxicity similar to that of **4** in dogs. In contrast, no hepatotoxicity or other major safety issues were observed in dogs for **5** (data not shown). Our studies indicate that a subtle and simple N/C exchange of phenyl with bioisosteric pyridinyl ("B" ring) can lead to a dramatically improved safety window *in vivo*. Our results also support the hypothesis that the bioactivation pathway of phenol **6** from **4** and **8** contributes to initiating a cascade of events leading toward the hepatotoxicity observed uniquely in dogs.

CONCLUSION

In summary, we described our detailed studies of AR pan-antagonist **4**, including impressive antitumor efficacy in an enzalutamide-resistant AR F877L LNCaP mouse xenograft model. Despite its attractive *in vitro* and *in vivo* pharmacological properties, idiopathic hepatotoxicity findings in dogs rendered **4** undevelopable. Metabolite identification studies revealed a latent bioactivation pathway associated with **4**. We hypothesized the link between *in vitro* bioactivation and *in vivo* toxicity by profiling close analogues of **4**. A simple bioisosteric C/N exchange from phenyl to pyridyl ("B" ring) was able to abolish the bioactivation. Our SAR studies led to the discovery of **5**, a clinical stage AR antagonist with improved safety margins and more balanced pharmacological profile.

With improved understanding of AR signaling in prostate cancer, there has been renewed interest in AR as a transcriptional factor.[37−41] For example, the discovery of the AR-V7 splicing variant is a useful biomarker but also represents a validated therapeutic target for novel drug discovery approaches.[9] Personalized treatment demands diversified cancer therapeutics in an era of precision medicine. The development of AR F877L antagonists such as **5** would provide an additional opportunity for the treatment of prostate cancer.[42]

EXPERIMENTAL SECTION

Chemistry. All commercial reagents and anhydrous solvents were purchased and used without further purification, unless otherwise specified. Mass spectra (MS) were obtained on a SHIMADZU LCMS-2020 MSD or Agilent 1200\G6110A MSD using electrospray ionization (ESI) in positive mode unless otherwise indicated. Calculated (calcd.) mass corresponds to the exact mass. Nuclear magnetic resonance (NMR) spectra were obtained on Bruker model AVIII 400 spectrometers. Definitions for multiplicity are as follows: s = singlet, d = doublet, t = triplet, q = quartet, dd = doublet of doublets, ddd = doublet of doublet of doublets, td = triplet of doublets, dt = doublet of triplets, spt = septet, quin = quintet, m = multiplet, br = broad. ^{1}H NMR chemical shifts are expressed in parts per million (δ) downfield from tetramethylsilane as a standard. Normal-phase silica gel chromatography (FCC) was performed on silica gel (SiO_2) using prepacked cartridges. Enzalutamide (**1** (MDV-3100)) was obtained from commercially available source. All compounds sent for biological tests were confirmed with purity >95% in quantitative HPLC analysis [method: Gilson GX-281-RP-HPLC with Phenomenex Gemini C18 (10 μm, 150 × 25 mm), or Waters XBridge C18 column (5 μm, 150 × 30 mm), mobile phase of 5−99% ACN in water (10 mM NH_4HCO_3) over 10 min and then held at 100% ACN for 2 min, at a flow rate of 25 mL/min] or elemental analysis in addition to LCMS and ^{1}H NMR.

Preparation of 5-(5-(4-Hydroxyphenyl)-8-oxo-6-thioxo-5,7-diazaspiro[3.4]octan-7-yl)-3-(trifluoromethyl)picolinonitrile (6). To a solution of l-((4-hydroxyphenyl)amino)cyclobutane-l-carbonitrile (19a, Supplementary Section S-9) (6.93 g, 29 mmol) in DMA (60 mL) was added solution of freshly prepared 5-isothiocyanato-3-(trifluoromethyl)picolinonitrile (**21a**, Supplementary Section S-9) (6.67 g, 29 mmol) in DMA (60 mL). The mixture was heated at 60 °C for overnight and then allowed to cool to room temperature. To the mixture was added with MeOH (58 mL) and aqueous HCl solution (1 M, 58 mL). The resulting reaction mixture was stirred at room temperature for 1 h. The mixture was diluted with ethyl acetate, washed with water, saturated aqueous $NaHCO_3$ solution, and brine. The organic layer was separated, and the aqueous layer was extracted with ethyl acetate. The combined organic extract was dried over $MgSO_4$, filtered, and concentrated. The residue was purified by chromatography (SiO_2, 0−65% EtOAc in heptane) to give the desired product, which was further purified by crystallization in acetonitrile to give the title compound as a white solid (7.9 g, 63%). mass calcd. for $C_{19}H_{13}F_3N_4O_2S$, 418.1; *m/z* found, 419.0 $[M + H]^+$; ^{1}H NMR (300 MHz, DMSO-d_6) δ 9.92 (s, 1H), 9.22 (d, J = 2.0 Hz, 1H), 8.76 (d, J = 2.0 Hz, 1H), 7.18 (d, J = 8.7 Hz, 2H), 6.95 (d, J = 8.7 Hz, 2H), 2.54−2.71 (m, 2H), 2.35−2.49 (m, 2H), 1.87−2.07 (m, 1H), 1.45−1.66 (m, 1H) ppm.

Preparation of 5-(5-(6-Hydroxypyridin-3-yl)-8-oxo-6-thioxo-5,7-diazaspiro[3.4]octan-7-yl)-3-(trifluoromethyl)-picolinonitrile (17). To a solution of 1-((6-hydroxypyridin-3-yl)amino)cyclobutanecarbonitrile (**19b**, Supplementary Section S-9S-9) (10.4 g, 54.5 mmol) in DMA (60 mL) was added a solution of 5-isothiocyanato-3-(trifluoromethyl)picolinonitrile (**21a**, Supplementary Section S-9) (13 g, 45.4 mmol) in DMA (60 mL). The mixture was heated at 60 °C for 2 h and then allowed to cool to room temperature. The mixture was treated with MeOH (100 mL) and HCl (2 M, 100 mL). The resulting suspension was stirred at 60 °C for 1 h. The mixture was filtered, and the filter cake was washed with water, MeOH, and then dried *in vacuo* to give the title compound as a gray solid (16.7 g, 86%). MS: mass calcd. for $C_{18}H_{12}F_3N_5O_2S$, 419.1; *m/z* found, 420.0 $[M + H]^+$; ^{1}H NMR (400 MHz, DMSO-*d6*) δ

https://dx.doi.org/10.1021/acs.jmedchem.0c01563
J. Med. Chem. 2021, 64, 909−924

12.01 (br s., 1H), 9.15 (s, 1H), 8.67 (s, 1H), 7.58 (br s, 1H), 7.40 (dd, J = 9.66, 2.32 Hz, 1H), 6.48 (d, J = 9.54 Hz, 1H), 2.53−2.60 (m, 2H), 2.36−2.44 (m, 2H), 1.88−2.01 (m, 1H), 1.60−1.71 (m, 1H) ppm.

Preparation of 5-(5-(4-hydroxyphenyl)-8-oxo-6-thioxo-5,7-diazaspiro[3.4]octan-7-yl)-3-methoxypicolinonitrile (22a). To a solution of l-((4-hydroxyphenyl)amino)cyclobutane-l-carbonitrile (**19a**, Supplementary Section S-9) (8.4 g, 44.7 mmol) in DMA (100 mL) was added a solution of 5-isothiocyanato-3-methoxypicolinonitrile (**21b**, Supplementary Section S-9) (10.3 g, 54 mmol) in DMA (100 mL). The mixture was heated at 60 °C for 1 h and then allowed to cool to room temperature. The mixture was treated with MeOH (45 mL) and HCl (1 M, 45 mL). The resulting suspension stirred at room temperature for overnight. Water (50 mL) was added, and the mixture was filtered. The precipitate was collected and dissolved into ethyl acetate (200 mL). The solution was washed with aqueous Na_2CO_3 solution, dried over $MgSO_4$, filtered, and concentrated. The product was dried *in vacuo* to give the title compound as a white solid (15 g, 88%). MS: mass calcd. for $C_{19}H_{16}N_4O_3S$, 380.1; m/z found, 381.1 $[M + H]^+$; ^1H NMR (400 MHz, $CDCl_3$) δ 8.43 (d, J = 1.98 Hz, 1H), 7.56 (d, J = 1.76 Hz, 1H), 7.14−7.22 (m, 2H), 6.97−7.06 (m, 2H), 5.13 (s, 1H), 4.00 (s, 3H), 2.61−2.71 (m, 2H), 2.50−2.60 (m, 2H), 2.17−2.29 (m, 1H), 1.63−1.73 (m, 1H) ppm.

Preparation of 5-(5-(6-Hydroxypyridin-3-yl)-8-oxo-6-thioxo-5,7-diazaspiro[3.4]octan-7-yl)-3-methoxypicolinonitrile (22b). To a solution of 1-((6-hydroxypyridin-3-yl)amino)-cyclobutanecarbonitrile (**19b**, Supplementary Section S-9) (7.3 g, 38.4 mmol) in DMA (50 mL) was added a solution of 5-isothiocyanato-3-methoxypicolinonitrile (**21b**, Supplementary Section S-9) (7.6 g, 32 mmol) in DMA (50 mL). The mixture was heated at 60 °C for 2 h and then allowed to cool to room temperature. The mixture was treated with MeOH (50 mL) and HCl (2 M, 50 mL). The resulting suspension was stirred at 60 °C for 2 h. Water (50 mL) was added, and the mixture was filtered. The precipitate was collected, washed with water and methanol, and dried *in vacuo* to give the title compound as a white solid (9 g, 74%). MS: mass calcd. for $C_{18}H_{15}N_5O_3S$, 381.1; m/z found, 382.1 $[M + H]^+$; ^1H NMR (300 MHz, DMSO-d_6) δ 12.02 (br s, 1H), 8.42 (d, J = 1.65 Hz, 1H), 8.00 (d, J = 1.65 Hz, 1H), 7.63 (d, J = 2.75 Hz, 1H), 7.45 (dd, J = 2.75, 9.90 Hz, 1H), 6.51 (d, J = 9.90 Hz, 1H), 4.00 (s, 3H), 2.27−2.73 (m, 4H), 1.85−2.13 (m, 1H), 1.59−1.80 (m, 1H) ppm.

Preparation of 5-(5-(6-Hydroxypyridin-3-yl)-8-oxo-6-thioxo-5,7-diazaspiro[3.4]octan-7-yl)-3-methylpicolinonitrile (22c). To a solution of 1-((6-hydroxypyridin-3-yl)amino)-cyclobutanecarbonitrile (**19b**, Supplementary Section S-9) (8.2 g, 43.3 mmol) in DMA (90 mL) was added a solution of 5-isothiocyanato-3-methylpicolinonitrile (**21c**, Supplementary Section S-9) (11.4 g, 65 mmol) in DMA (90 mL). The mixture was heated at 60 °C for 4 h and then allowed to cool to room temperature. The mixture was treated with MeOH (90 mL) and HCl (1 M, 87 mL). The resulting suspension was stirred at room temperature for 1 h. The mixture was diluted with ethyl acetate, washed with water, saturated aqueous $NaHCO_3$ solution, and brine. The organic layer was separated, and the aqueous layer was extracted with ethyl acetate. The combined organic extract was dried over $MgSO_4$, filtered, and concentrated. The residue was purified by chromatography (SiO_2, 0−65% EtOAc in heptane) to give the desired product, which was further purified by crystallization in acetonitrile to give the title compound as a brown solid (12.8 g, 69%). MS: mass calcd. for $C_{18}H_{15}N_5O_2S$, 365.1; m/z found, 366.1 $[M + H]^+$; ^1H NMR (400 MHz, $CDCl_3$) δ 13.20 (br s, 1H), 8.66 (d, J = 1.98 Hz, 1H), 7.82 (d, J = 1.76 Hz, 1H), 7.48 (d, J = 2.65 Hz, 1H), 7.42 (dd, J = 9.70, 2.65 Hz, 1H), 6.75 (d, J = 9.70 Hz, 1H), 2.61−2.75 (m, 5H), 2.43−2.56 (m, 2H), 2.25−2.37 (m, 1H), 1.77−1.89 (m, 1H) ppm.

Preparation of 3-Chloro-5-(5-(6-hydroxypyridin-3-yl)-8-oxo-6-thioxo-5,7-diazaspiro[3.4]octan-7-yl)picolinonitrile (22d). To a solution of 1-((6-hydroxypyridin-3-yl)amino)-cyclobutanecarbonitrile (**19b**, Supplementary Section S-9) (10.9 g, 57.3 mmol) in DMA (50 mL) was added a solution of 3-chloro-5-isothiocyanatopicolinonitrile (**21d**, Supplementary Section S-9) (14 g, 57.3 mmol) in DMA (50 mL). The mixture was heated at 60 °C for 2 h and then allowed to cool to room temperature. The mixture was treated with MeOH (100 mL) and HCl (2 M, 100 mL). The resulting suspension was stirred at 60 °C for 2 h. The mixture was cooled to room temperature, and water (100 mL) was added. The precipitate was collected by filtration, washed with water and methanol, and dried *in vacuo* to give the title compound as a white solid (15 g, 66%). MS: mass calcd. for $C_{17}H_{12}ClN_5O_2S$, 385.0; m/z found, 386.0 $[M + H]^+$; ^1H NMR (400 MHz, DMSO-d_6) δ 11.96 (br s, 1H), 8.83 (d, J = 1.96 Hz, 1H), 8.47 (d, J = 1.96 Hz, 1H), 7.58 (d, J = 2.45 Hz, 1H), 7.40 (dd, J = 9.66, 2.81 Hz, 1H), 6.48 (d, J = 9.78 Hz, 1H), 2.50−2.62 (m, 2H), 2.36−2.45 (m, 2H), 1.88−2.03 (m, 1H), 1.57−1.73 (m, 1H) ppm.

Preparation of 3-Chloro-5-(5-(4-hydroxyphenyl)-8-oxo-6-thioxo-5,7-diazaspiro[3.4]octan-7-yl)picolinonitrile (22e). To a solution of l-((4-hydroxyphenyl)amino)cyclobutane-l-carbonitrile (**19a**, Supplementary Section S-9) (11 g, 58.6 mmol) in DMA (50 mL) was added a solution of 3-chloro-5-isothiocyanatopicolinonitrile (**21d**, Supplementary Section S-9) (11.9 g, 48.8 mmol) in DMA (50 mL). The mixture was heated at 60 °C for 2 h and then allowed to cool to room temperature. The mixture was treated with MeOH (100 mL) and HCl (2 M, 100 mL). The resulting suspension was stirred at 60 °C for 2 h. The mixture was cooled to room temperature, and water (100 mL) was added. The precipitate was collected by filtration, washed with water and methanol, and dried *in vacuo* to give the title compound as a white solid (17 g, 90%). MS: mass calcd. for $C_{18}H_{13}ClN_4O_2S$, 384.0; m/z found, 385.0 $[M + H]^+$; ^1H NMR (400 MHz, DMSO-d_6) δ 9.93 (s, 1H), 8.90 (d, J = 2.01 Hz, 1H), 8.54 (d, J = 2.01 Hz, 1H), 7.18 (d, J = 8.78 Hz, 2H), 6.94 (d, J = 8.78 Hz, 2H), 2.54−2.65 (m, 2H), 2.38−2.46 (m, 2H), 1.89−2.01 (m, 1H), 1.48−1.60 (m, 1H) ppm.

Preparation of 5-(5-(4-((1-Methylpiperidin-4-yl)oxy)-phenyl)-8-oxo-6-thioxo-5,7-diazaspiro[3.4]octan-7-yl)-3-(trifluoromethyl)picolinonitrile (4). To a mixture of 5-(5-(4-hydroxyphenyl)-8-oxo-6-thioxo-5,7-diazaspiro[3.4]octan-7-yl)-3-methoxypicolinonitrile (6) (6.3 g, 15 mmol), 1-methylpiperidin-4-ol (2.1 g, 18 mmol), and triphenylphosphine (7.9 g, 30 mmol) in anhydrous THF (150 mL) was added diethyl azodicarboxylate (DEAD, 5.2 g, 30 mmol) dropwise over a period of 15−20 min under nitrogen. Upon completion of the addition, the reaction mixture was stirred at room temperature for 5 h. The mixture was concentrated. The crude residue was purified by chromatography (SiO_2, 0−10% MeOH in EtOAc) to give the desired product. The solid was dissolved into 1,4-dioxane (40 mL), and a 1,4-dioxane (4 M) solution of HCl (2.8 mL, 11.2 mmol) was added. The mixture was stirred at room temperature for 2 h and then concentrated. The residue was triturated in diethyl ether (200 mL) for overnight. The precipitate was collected by filtration, washed with diethyl ether, and dried *in vacuo* to give the title compound as a HCl salt: a white solid (5.83 g, 70%). LCMS (API): mass calcd. for $C_{25}H_{24}F_3N_5O_2S{\cdot}HCl$, 515.2; m/z found, 516.1 $[M + H]^+$; ^1H NMR (300 MHz, DMSO-d_6) δ 9.23 (d, J = 1.10 Hz, 1H), 8.77 (d, J = 1.65 Hz, 1H), 7.31 (d, J = 8.80 Hz, 2H), 7.16 (d, J = 8.80 Hz, 2H), 4.47 (td, J = 4.26, 7.97 Hz, 1H), 2.54−2.77 (m, 5H), 2.38−2.50 (m, 2H), 2.28 (br s, 1H), 2.20−2.32 (m, 1H), 2.24 (s, 3H), 1.92−2.06 (m, 3H), 1.63−1.80 (m, 2H), 1.49−1.64 (m, 1H) ppm. Anal. Calcd for $C_{25}H_{24}F_3N_5O_2S$: C, 58.24; H, 4.69; N, 13.58. Found: C, 57.99; H, 4.47; N, 13.33.

Preparation of 3-Methoxy-5-(5-(4-((1-methylpiperidin-4-yl)-oxy)phenyl)-8-oxo-6-thioxo-5,7-diazaspiro[3.4]octan-7-yl)-picolinonitrile (11). To a mixture of 5-(5-(4-hydroxyphenyl)-8-oxo-6-thioxo-5,7-diazaspiro[3.4]octan-7-yl)-3-methoxypicolinonitrile (**22a**) (9 g, 23.7 mmol), 1-methylpiperidin-4-ol (5.4 g, 47.3 mmol), and triphenylphosphine (12.4 g, 47.3 mmol) in anhydrous THF (150 mL) was added diethyl azodicarboxylate (DEAD, 8.2 g, 47.3 mmol) dropwise over a period of 15−20 min under nitrogen. Upon completion of the addition, the reaction mixture was stirred at 30 °C for overnight. The mixture was concentrated. The crude residue was purified by chromatography (SiO_2, 0−20% MeOH in EtOAc) to give the desired product as a yellow solid. The solid was dissolved into 1,4-dioxane (60 mL), and a 1,4-dioxane (4 M) solution of HCl (4.2

https://dx.doi.org/10.1021/acs.jmedchem.0c01563
J. Med. Chem. 2021, 64, 909−924

mL, 16.8 mmol) was added. The mixture was stirred at room temperature for 2 h and then concentrated. The residue was triturated in diethyl ether (250 mL) for overnight. The precipitate was collected by filtration, washed with diethyl ether, and dried *in vacuo* to give the title compound as a HCl salt: a white solid (6.86 g, 56%). LCMS (API): mass calcd. for $C_{25}H_{27}N_5O_3S$·HCl, 477.2; *m/z* found, 478.0 $[M + H]^+$; ^1H NMR (300 MHz, DMSO-d_6) δ 10.17 (br s, 1H), 8.45 (d, J = 1.7 Hz, 1H), 8.04 (d, J = 1.8 Hz, 1H), 7.35 (d, J = 8.4 Hz, 2H), 7.21 (d, J = 8.4 Hz, 2H), 4.57−4.90 (m, 1H), 3.99 (s, 3H), 3.43−3.61 (m, 1H), 3.29−3.36 (m, 1H), 3.00−3.27 (m, 2H), 2.79 (br s, 3H), 2.56−2.68 (m, 2H), 2.36−2.46 (m, 2H), 2.23−2.36 (m, 1H), 2.04−2.19 (m, 2H), 1.77−2.04 (m, 2H), 1.44−1.63 (m, 1H) ppm. Anal. Calcd for $C_{25}H_{24}F_3N_5O_2S$·HCl·H_2O: C, 56.44; H, 5.68; N, 13.16. Found: C, 56.40; H, 5.70; N, 12.72.

Preparation of 3-Methoxy-5-(5-(6-((1-methylpiperidin-4-yl)-oxy)pyridin-3-yl)-8-oxo-6-thioxo-5,7-diazaspiro[3.4]octan-7-yl)picolinonitrile (12). To a mixture of 5-(5-(6-hydroxypyridin-3-yl)-8-oxo-6-thioxo-5,7-diazaspiro[3.4]octan-7-yl)-3-methoxypicolinonitrile (**22b**) (6.87 g, 18 mmol), 1-methylpiperidin-4-ol (4.1 g, 36 mmol), and triphenylphosphine (9.4 g, 36 mmol) in anhydrous THF (150 mL) was added diethyl azodicarboxylate (DEAD, 6.27 g, 36 mmol) dropwise over a period of 15−20 min under nitrogen. Upon completion of the addition, the reaction mixture was stirred at 30 °C for overnight. The mixture was concentrated. The crude residue was purified by chromatography (SiO_2, 0−20% MeOH in EtOAc) to give the desired product as a yellow solid. The solid was dissolved into 1,4-dioxane (40 mL), and a 1,4-dioxane (4 M) solution of HCl (3 mL, 12 mmol) was added. The mixture was stirred at room temperature for 2 h and then concentrated. The residue was triturated in diethyl ether (200 mL) for overnight. The precipitate was collected by filtration, washed with diethyl ether, and dried *in vacuo* to give the title compound as a HCl salt: a beige solid (5.5 g, 62%). LCMS (API): mass calcd. for $C_{24}H_{26}N_6O_3S$·HCl, 478.2; *m/z* found, 479.1 $[M + H]^+$; ^1H NMR (300 MHz, DMSO-d_6) δ 10.62 (br s, 1H), 8.45 (d, J = 1.8 Hz, 1H), 8.24 (dd, J = 4.5, 2.5 Hz, 1H), 8.04 (d, J = 1.8 Hz, 1H), 7.82 (ddd, J = 9.0, 6.6, 2.5 Hz, 1H), 7.07 (dd, J = 8.8, 4.1 Hz, 1H), 5.16−5.42 (m, 1H), 3.99 (s, 3H), 3.42−3.54 (m, 1H), 3.30−3.42 (m, 1H), 3.05−3.28 (m, 2H), 2.78 (dd, J = 11.6, 4.6 Hz, 3H), 2.57−2.71 (m, 2H), 2.37−2.46 (m, 2H), 2.22−2.37 (m, 1H), 2.11−2.24 (m, 2H), 1.86−2.10 (m, 2H), 1.47−1.70 (m, 1H) ppm. Anal. Calcd for $C_{24}H_{26}N_6O_3S$·HCl·H_2O: C, 54.08; H, 5.48; N, 15.77. Found: C, 53.71; H, 5.26; N, 15.32.

Preparation of 5-(8-Oxo-5-(4-(piperidin-4-yloxy)phenyl)-6-thioxo-5,7-diazaspiro[3.4]octan-7-yl)-3-(trifluoromethyl)-picolinonitrile (8). Step A. To a mixture of 5-(5-(4-hydroxyphenyl)-8-oxo-6-thioxo-5,7-diazaspiro[3.4]octan-7-yl)-3-(trifluoromethyl)-picolinonitrile (**6**) (25 g, 59.7 mmol), *tert*-butyl 4-hydroxypiperidine-1-carboxylate (18.6 g, 89.7 mmol), and triphenylphosphine (31.4 g, 120 mmol) in anhydrous THF (400 mL) was added a solution of diisopropyl azodicarboxylate (DIAD, 23.5 mL, 120 mmol) in anhydrous THF (250 mL) dropwise over a period of 30 min under nitrogen. Upon completion of the addition, the reaction mixture was stirred at room temperature for 0.5 h. The mixture was concentrated. The crude residue was purified by chromatography (SiO_2, 0−60% EtOAc in heptane) to give the crude product, which was further purified by reverse phase chromatography [C18 colomn, Start (90% H_2O-10% ACN-MeOH)-End (54% H_2O-46% ACN-MeOH-0.1% HCOOH)]. The product was neutralized with Na_2CO_3 solution and then extracted with DCM. The organic extract was separated, dried over $MgSO_4$, filtered, and concentrated. The residue was triturated in diethyl ether to give *tert*-butyl 4-(4-(7-(6-cyano-5-(trifluoromethyl)-pyridin-3-yl)-8-oxo-6-thioxo-5,7-diazaspiro[3.4]octan-5-yl)phenoxy)-piperidine-1-carboxylate as a white foam (18 g, 49%). LCMS (API): mass calcd. for $C_{29}H_{30}F_3N_5O_4S$, 601.2; *m/z* found, 602.1 $[M + H]^+$; ^1H NMR (400 MHz, $CDCl_3$) δ 9.11 (d, J = 2.26 Hz, 1H), 8.37 (d, J = 2.26 Hz, 1H), 7.22 (d, J = 8.78 Hz, 2H), 7.08 (d, J = 8.78 Hz, 2H), 4.56 (d, J = 3.01 Hz, 1H), 3.67−3.79 (m, 2H), 3.34−3.44 (m, 2H), 2.51−2.73 (m, 4H), 2.19−2.30 (m, 1H), 1.97 (br s, 2H), 1.83 (d, J = 3.01 Hz, 2H), 1.70 (d, J = 10.79 Hz, 1H), 1.49 (s, 9H) ppm. Step B. To *tert*-butyl 4-(4-(7-(6-cyano-5-(trifluoromethyl)pyridin-3-yl)-8-oxo-6-thioxo-5,7-diazaspiro[3.4]octan-5-yl)phenoxy)piperidine-1-carboxylate (8 g, 13 mmol) in DCM (130 mL) was added TFA (14 mL). The reaction mixture was stirred at room temperature for 2 h. The mixture concentrated, and toluene was added to the residue. The solvent was evaporated, and the remaining mixture was poured into aqueous saturated $NaHCO_3$ and extracted with EtOAc. The organic layer was washed with water, brine, dried over $MgSO_4$, filtered, and concentrated. The crude material was purified by chromatography (SiO_2, 0−10% MeOH in DCM) to provide the desired product (6.86 g). The product was dissolved into 1,4-dioxane (50 mL), and a 1,4-dioxane solution (4 M) of HCl (3.3 mL, 13.2 mmol) was added. The mixture was stirred at room temperature for 1 h and then concentrated. The residue was triturated in diethyl ether, and the precipitate was collected, washed with diethyl ether, and dried *in vacuo* to give the title compound as a HCl salt: white solid (6.08 g, 86%). LCMS (API): mass calcd. for $C_{24}H_{22}F_3N_5O_2S$·HCl, 501.1; *m/z* found, 502.1 $[M + H]^+$; ^1H NMR (400 MHz, $CDCl_3$) δ 9.65 (br s, 2H), 9.09 (s, 1H), 8.35 (s, 1H), 7.21−7.26 (m, 2H), 7.08 (d, J = 7.58 Hz, 2H), 4.76 (br s, 1H), 3.40 (br s, 4H), 2.67 (d, J = 8.80 Hz, 2H), 2.49−2.62 (m, 2H), 2.38 (br s, 2H), 2.24 (d, J = 9.05 Hz, 3H), 1.69 (d, J = 10.03 Hz, 1H) ppm.

Preparation of 5-(8-Oxo-5-(6-(piperidin-4-yloxy)pyridin-3-yl)-6-thioxo-5,7-diazaspiro[3.4]octan-7-yl)-3-(trifluoromethyl)-picolinonitrile (5). Step A. To a mixture of 5-(5-(6-hydroxypyridin-3-yl)-8-oxo-6-thioxo-5,7-diazaspiro[3.4]octan-7-yl)-3-(trifluoromethyl)picolinonitrile (17) (16.6 g, 39.6 mmol), *tert*-butyl 4-hydroxypiperidine-1-carboxylate (8.94 g, 43.5 mmol), and triphenylphosphine (22.8 g, 87.1 mmol) in anhydrous THF (150 mL) was added a solution of diisopropyl azodicarboxylate (DIAD, 15.6 mL, 79.1 mmol) in anhydrous THF (50 mL) dropwise over a period of 10 min under nitrogen. Upon completion of the addition, the reaction mixture was stirred at 50 °C for 3 h. The mixture was cooled to room temperature and concentrated. The crude residue was purified by chromatography (SiO_2, 0−30% EtOAc in heptane) to give crude *tert*-butyl 4-((5-(7-(6-cyano-5-(trifluoromethyl)pyridin-3-yl)-8-oxo-6-thioxo-5,7-diazaspiro[3.4]octan-5-yl)pyridin-2-yl)oxy)piperidine-1-carboxylate as an amorphous foam (43.4 g), which was used directly to next step without further purification. MS: mass calcd. for $C_{28}H_{29}F_3N_6O_4S$, 602.2; *m/z* found, 547.1 $[M + H\text{-}tBu]^+$; ^1H NMR (300 MHz, $CDCl_3$) δ 9.09 (d, J = 2.2 Hz, 1H), 8.36 (d, J = 2.2 Hz, 1H), 8.09 (d, J = 2.6 Hz, 1H), 7.52 (dd, J = 8.8, 2.6 Hz, 1H), 6.91 (d, J = 8.8 Hz, 1H), 5.21−5.35 (m, 1H), 3.70−3.90 (m, 2H), 3.22−3.40 (m, 2H), 2.63−2.80 (m, 2H), 2.44−2.62 (m, 2H), 2.15−2.35 (m, 1H), 1.94−2.10 (m, 2H), 1.66−1.86 (m, 3H), 1.47 (s, 9H) ppm.

Step B. To a solution of crude *tert*-butyl 4-((5-(7-(6-cyano-5-(trifluoromethyl)pyridin-3-yl)-8-oxo-6-thioxo-5,7-diazaspiro[3.4]-octan-5-yl)pyridin-2-yl)oxy)piperidine-1-carboxylate (43.4 g) in DCM (300 mL) was added TFA (60 mL). The reaction mixture was stirred at room temperature for overnight. The mixture concentrated, and the residue was taken in toluene (150 mL) and again concentrated (three times). The crude residue was then purified by column chromatography on silica gel (gradient of MeOH in DCM from 0 to 10%) to afford a yellowish amorphous solid (19.8 g). Final purification was performed by preparative LC (gradient of a mixture ACN/MeOH (1/1, v/v) in 0.1% aqueous formic acid from 10 to 54%). The pure fractions were collected, and the "pH" was brought to 8−9 by addition of solid Na_2CO_3. The product was extracted with ethyl acetate (3 × 400 mL). The combined organic layers were washed with brine (300 mL), dried over $MgSO_4$, filtered, and concentrated to give 5-(8-oxo-5-(6-(piperidin-4-yloxy)pyridin-3-yl)-6-thioxo-5,7-diazaspiro[3.4]octan-7-yl)-3-(trifluoromethyl)-picolinonitrile (**5**) as a white foam (9.57 g, 47% for two steps). MS: mass calcd. for $C_{23}H_{21}F_3N_6O_2S$, 502.1; *m/z* found, 503.1 $[M + H]^+$; ^1H NMR (300 MHz, $CDCl_3$) δ 8.91 (d, J = 2.2 Hz, 1H), 8.24 (d, J = 2.2 Hz, 1H), 7.90 (d, J = 2.6 Hz, 1H), 7.39 (dd, J = 8.7, 2.6 Hz, 1H), 6.74 (d, J = 8.7 Hz, 1H), 5.15−5.27 (m, 1H), 3.10−3.30 (m, 2H), 2.94−3.09 (m, 2H), 2.42−2.60 (m, 2H), 2.20−2.41 (m, 2H), 1.87−2.15 (m, 5H), 1.45−1.57 (m, 1H) ppm.

Step C. 5-(8-oxo-5-(6-(piperidin-4-yloxy)pyridin-3-yl)-6-thioxo-5,7-diazaspiro[3.4]octan-7-yl)-3-(trifluoromethyl)picolinonitrile (**5**)

https://dx.doi.org/10.1021/acs.jmedchem.0c01563
J. Med. Chem. 2021, 64, 909−924

(9.57 g, 19.0 mmol) was dissolved into 1,4-dioxane (54 mL), and a 1,4-dioxane solution (4 M) of HCl (5.24 mL, 20.9 mmol) was added. The mixture was stirred at room temperature for 1 h and then concentrated. The residue was triturated in diethyl ether (50 mL) for overnight. The precipitate was collected by filtration through a sintered funnel, washed with diethyl ether (2 × 15 mL), and dried *in vacuo* to give the title compound as a HCl salt: a white solid (9.85 g, 93%). LCMS (API): mass calcd. for $C_{23}H_{21}F_3N_6O_2S$·HCl, 502.1; *m/z* found, 503.1 $[M + H]^+$; ^1H NMR (300 MHz, DMSO-d_6) δ 9.21 (d, J = 2.0 Hz, 1H), 8.92 (br s, 2H), 8.75 (d, J = 2.0 Hz, 1H), 8.22 (d, J = 2.6 Hz, 1H), 7.80 (dd, J = 8.8, 2.6 Hz, 1H), 7.09 (d, J = 8.8 Hz, 1H), 5.26−5.40 (m, Hz, 1H), 3.21−3.35 (m, 2H), 3.04−3.20 (m, 2H), 2.58−2.73 (m, 2H), 2.34−2.48 (m, 2H), 2.12−2.29 (m, 2H), 1.87−2.04 (m, 3H), 1.48−1.69 (m, 1H) ppm; Anal. Calcd for $C_{23}H_{21}F_3N_6O_2S$·HCl: C, 51.26; H, 4.11; N, 15.59; Found: C, 51.02; H, 4.01; N, 15.57.

Preparation of 3-Methyl-5-(8-oxo-5-(6-(piperidin-4-yloxy)-pyridin-3-yl)-6-thioxo-5,7-diazaspiro[3.4]octan-7-yl)-picolinonitrile (13). Step A. To a mixture of 5-(5-(6-hydroxypyridin-3-yl)-8-oxo-6-thioxo-5,7-diazaspiro[3.4]octan-7-yl)-3-(trifluoromethyl)picolinonitrile (17) (12.8 g, 35 mmol), *tert*-butyl 4-hydroxypiperidine-1-carboxylate (8.46 g, 32 mmol), and triphenylphosphine (16.5 g, 63 mmol) in anhydrous THF (125 mL) was added a solution of diisopropyl azodicarboxylate (DIAD, 12.4 mL, 63 mmol) in anhydrous THF (250 mL) dropwise over a period of 30 min under nitrogen. Upon completion of the addition, the reaction mixture was stirred at 50 °C for 2 h. The mixture was cooled to room temperature and concentrated. The residue was triturated in a mixture of ethyl acetate and heptane. The precipitate of triphenylphosphine oxide was filtered, and the filtrate was concentrated. The crude residue was purified by chromatography (SiO_2, 0−45% EtOAc in heptane) to give *tert*-butyl 4-((5-(7-(6-cyano-5-methylpyridin-3-yl)-8-oxo-6-thioxo-5,7-diazaspiro[3.4]octan-5-yl)pyridin-2-yl)oxy)-piperidine-1-carboxylate as a yellow foam (14.9 g, 77%). MS: mass calcd. for $C_{28}H_{32}N_6O_4S$, 548.2; *m/z* found, 493.1 $[M + H\text{-}tBu]^+$; ^1H NMR (300 MHz, DMSO-d_6) δ 8.66−8.77 (m, 1H), 8.24 (d, J = 2.20 Hz, 1H), 8.15 (s, 1H), 7.79 (dd, J = 2.75, 8.80 Hz, 1H), 7.04 (d, J = 8.80 Hz, 1H), 5.17−5.34 (m, 1H), 3.67−3.85 (m, 2H), 3.08−3.27 (m, 2H), 2.62−2.72 (m, 1H), 2.35−2.54 (m, 5H), 1.90−2.12 (m, 3H), 1.51−1.72 (m, 3H), 1.43 (s, 9H), 1.19−1.32 (m, 1H) ppm.

Step B. To a solution of *tert*-butyl 4-((5-(7-(6-cyano-5-methylpyridin-3-yl)-8-oxo-6-thioxo-5,7-diazaspiro[3.4]octan-5-yl)pyridin-2-yl)-oxy)piperidine-1-carboxylate (14.9 g, 27 mmol) in DCM (110 mL) was added TFA (54 mL). The reaction mixture was stirred at room temperature for 1 h. The mixture concentrated, and the residue was taken in toluene (150 mL) and again concentrated (3 × 50 mL). The crude residue was diluted with DCM (500 mL) and washed with aqueous Na_2CO_3 solution (1 M, 250 mL). The organic layer was separated, and aqueous layer was extracted with DCM (500 mL). The combined organic extract was dried over $MgSO_4$, filtered, and concentrated. The residue was purified by chromatography (SiO_2, MeOH in DCM from 0 to 10%) to afford a yellowish amorphous solid. Final purification was performed by preparative LC ([Start (90% H_2O-10% ACN)-End (54% H_2O-46% ACN]-[25 mM NH_4HCO_3]). The pure fractions were collected, and brine was added (200 mL). The mixture was extracted with DCM (200 mL). The organic layer was separated, dried over $MgSO_4$, filtered, and concentrated to give 3-methyl-5-(8-oxo-5-(6-(piperidin-4-yloxy)-pyridin-3-yl)-6-thioxo-5,7-diazaspiro[3.4]octan-7-yl)picolinonitrile (**13**) as a yellow solid (8.56 g, 69% for two steps). MS: mass calcd. for $C_{23}H_{24}N_6O_2S$, 448.2; *m/z* found, 449.1 $[M + H]^+$; ^1H NMR (300 MHz, DMSO-d_6) δ 8.99 (br s, 2H), 8.71 (d, J = 2.1 Hz, 1H), 8.23 (d, J = 2.6 Hz, 1H), 8.13 (d, J = 2.2 Hz, 1H), 7.82 (dd, J = 8.8, 2.6 Hz, 1H), 7.07 (d, J = 8.8 Hz, 1H), 5.20−5.40 (m, 1H), 3.20−3.36 (m, 2H), 3.02−3.20 (m, 2H), 2.55−2.70 (m, 2H), 2.29−2.47 (m, 2H), 2.11−2.29 (m, 2H), 1.84−2.06 (m, 3H), 1.49−1.69 (m, 1H) ppm.

Step C. 3-methyl-5-(8-oxo-5-(6-(piperidin-4-yloxy)pyridin-3-yl)-6-thioxo-5,7-diazaspiro[3.4]octan-7-yl)picolinonitrile (**13**) (8.56 g, 19.0 mmol) was dissolved into 1,4-dioxane (75 mL), and a 1,4-dioxane solution (4 M) of HCl (5.25 mL, 21 mmol) was added. The mixture was stirred at room temperature for 4 h and then concentrated. The yellow solid was triturated in diethyl ether (100 mL) for overnight. The precipitate was collected by filtration through a sintered funnel, washed with diethyl ether, and dried *in vacuo* to give the title compound as a HCl salt: a white solid (8.62 g, 91%). LCMS (API): mass calcd. for $C_{23}H_{24}N_6O_2S$·HCl, 448.2; *m/z* found, 449.1 $[M + H]^+$; ^1H NMR (300 MHz, DMSO-d_6) δ 8.88−9.16 (m, 2H), 8.72 (d, J = 1.65 Hz, 1H), 8.25 (d, J = 2.20 Hz, 1H), 8.14 (d, J = 1.65 Hz, 1H), 7.83 (dd, J = 2.20, 8.80 Hz, 1H), 7.08 (d, J = 8.80 Hz, 1H), 5.21−5.43 (m, 1H), 3.27 (br s, 2H), 3.14 (br d, J = 3.85 Hz, 2H), 2.60−2.70 (m, 2H), 2.59 (s, 3H), 2.35−2.49 (m, 2H), 2.12−2.29 (m, 2H), 1.86−2.08 (m, 3H), 1.47−1.71 (m, 1H) ppm.

Preparation of 3-Chloro-5-(8-oxo-5-(6-(piperidin-4-yloxy)-pyridin-3-yl)-6-thioxo-5,7-diazaspiro[3.4]octan-7-yl)-picolinonitrile (14). Step A. To a mixture of 3-chloro-5-(5-(6-hydroxypyridin-3-yl)-8-oxo-6-thioxo-5,7-diazaspiro[3.4]octan-7-yl)-picolinonitrile (**22d**) (5 g, 12.9 mmol), *tert*-butyl 4-hydroxypiperidine-1-carboxylate (3.9 g, 19 mmol), and triphenylphosphine (6.1 g, 23 mmol) in anhydrous THF (25 mL) was added a solution of diisopropyl azodicarboxylate (DIAD, 4.6 mL, 23 mmol) in anhydrous THF (25 mL) dropwise over a period of 10 min under nitrogen. Upon completion of the addition, the reaction mixture was stirred at 50 °C for 2 h. The mixture was cooled to room temperature and concentrated. The residue was triturated in a mixture of ethyl acetate and heptane. The precipitate of triphenylphosphine oxide was filtered, and the filtrate was concentrated. The crude residue was purified by chromatography (SiO_2, 0−30% EtOAc in heptane) to give *tert*-butyl 4-((5-(7-(5-chloro-6-cyanopyridin-3-yl)-8-oxo-6-thioxo-5,7-diazaspiro[3.4]octan-5-yl)pyridin-2-yl)oxy)piperidine-1-carboxylate as a yellow foam (7.6 g, 100%). MS: mass calcd. for $C_{27}H_{29}ClN_6O_4S$, 568.2; *m/z* found, 513.0 $[M + H\text{-}tBu]^+$; ^1H NMR (300 MHz, $CDCl_3$) δ 8.76−8.82 (m, 1H), 8.09 (dd, J = 9.66, 2.32 Hz, 2H), 7.50 (dd, J = 8.68, 2.81 Hz, 1H), 6.90 (d, J = 8.80 Hz, 1H), 5.28 (tt, J = 7.89, 3.97 Hz, 1H), 3.74−3.85 (m, 2H), 3.30 (ddd, J = 13.27, 8.99, 3.67 Hz, 2H), 2.62−2.75 (m, 2H), 2.43−2.57 (m, 2H), 2.19−2.33 (m, 1H), 2.02 (d, J = 9.05 Hz, 2H), 1.70−1.83 (m, 3H), 1.47 (s, 9H) ppm.

Step B. To a solution of *tert*-butyl 4-((5-(7-(5-chloro-6-cyanopyridin-3-yl)-8-oxo-6-thioxo-5,7-diazaspiro[3.4]octan-5-yl)-pyridin-2-yl)oxy)piperidine-1-carboxylate (7.4 g, 13 mmol) in DCM (65 mL) was added TFA (14 mL). The reaction mixture was stirred at room temperature for 2 h. The mixture concentrated and toluene was added to the residue. The solvent was evaporated, and the remaining mixture was poured into aqueous saturated $NaHCO_3$ and extracted with EtOAc. The organic layer was washed with water, brine, dried over $MgSO_4$, filtered, and concentrated. The crude material was purified by chromatography (SiO_2, 0−10% MeOH in DCM) to provide the desired product. The product was dissolved into 1,4-dioxane (50 mL), and a 1,4-dioxane solution (4 M) of HCl (10 mL, 40 mmol) was added. The mixture was stirred at room temperature for 1 h and then concentrated. The residue was triturated in diethyl ether, and the precipitate was collected, washed with diethyl ether, and dried *in vacuo* to give the title compound as a HCl salt: a white solid (4.95 g, 78%). LCMS (API): mass calcd. for $C_{22}H_{21}ClN_6O_2S$·HCl, 468.1; *m/z* found, 468.9 $[M + H]^+$; ^1H NMR (300 MHz, DMSO-d_6) δ 9.23 (s, 2H), 8.91 (d, J = 2.0 Hz, 1H), 8.55 (d, J = 2.1 Hz, 1H), 8.24 (d, J = 2.6 Hz, 1H), 7.81 (dd, J = 8.8, 2.6 Hz, 1H), 7.09 (d, J = 8.8 Hz, 1H), 5.28−5.37 (m, 1H), 3.07−3.31 (m, 4H), 2.59−2.71 (m, 2H), 2.39−2.47 (m, 2H), 2.17−2.31 (m, 2H), 1.93−2.05 (m, 3H), 1.59 (d, J = 10.7 Hz, 1H) ppm.

Preparation of 3-Chloro-5-(8-oxo-5-(4-(piperidin-4-yloxy)-phenyl)-6-thioxo-5,7-diazaspiro[3.4]octan-7-yl)picolinonitrile (15). Step A. To a mixture of 3-chloro-5-(5-(4-hydroxyphenyl)-8-oxo-6-thioxo-5,7-diazaspiro[3.4]octan-7-yl)picolinonitrile (**22e**) (4.15 g, 10.1 mmol), *tert*-butyl 4-hydroxypiperidine-1-carboxylate (3.16 g, 15.2 mmol), and triphenylphosphine (5.3 g, 20.2 mmol) in anhydrous toluene (35 mL) and DMF (5 mL) was added a solution of diisopropyl azodicarboxylate (DIAD, 4.4 mL, 22 mmol) in anhydrous toluene (15 mL) dropwise over a period of 10 min under nitrogen. Upon completion of the addition, the reaction mixture was stirred at 50 °C for 1 h. The mixture was cooled to room temperature and

https://dx.doi.org/10.1021/acs.jmedchem.0c01563
J. Med. Chem. 2021, 64, 909−924

concentrated. The residue was triturated in a mixture of ethyl acetate and heptane. The precipitate of triphenylphosphine oxide was filtered, and the filtrate was concentrated. The crude residue was purified by chromatography (SiO_2, 0−65% EtOAc in heptane) to give crude *tert*-butyl 4-(4-(7-(5-chloro-6-cyanopyridin-3-yl)-8-oxo-6-thioxo-5,7-diazaspiro[3.4]octan-5-yl)phenoxy)piperidine-1-carboxylate as a white foam (5.7 g, 100%). MS: mass calcd. for $C_{28}H_{30}ClN_5O_4S$, 567.2; *m/z* found, 512.1 $[M+H\text{-}tBu]^+$; ^1H NMR (400 MHz, DMSO-d_6) δ 8.88 (d, J = 1.47 Hz, 1H), 8.52 (d, J = 1.47 Hz, 1H), 7.29 (d, J = 8.56 Hz, 2H), 7.16 (d, J = 8.80 Hz, 2H), 4.62 (br s, 1H), 3.63−3.78 (m, 2H), 3.18 (br s, 2H), 2.54−2.66 (m, 2H), 2.33−2.45 (m, 2H), 1.88−2.04 (m, 3H), 1.48−1.65 (m, 3H), 1.40 (s, 9H), ppm.

Step B. To a solution of *tert*-butyl *tert*-butyl 4-(4-(7-(5-chloro-6-cyanopyridin-3-yl)-8-oxo-6-thioxo-5,7-diazaspiro[3.4]octan-5-yl)-phenoxy)piperidine-1-carboxylate (5.7 g, 10 mmol) in DCM (100 mL) was added TFA (10 mL). The reaction mixture was stirred at room temperature for 2 h. The mixture concentrated and toluene was added to the residue. The solvent was evaporated, and the remaining mixture was poured into aqueous saturated $NaHCO_3$ and extracted with DCM. The organic layer was washed with water, brine, dried over $MgSO_4$, filtered, and concentrated. The crude material was purified by chromatography (SiO_2, 0−10% MeOH in DCM) to provide the desired product. The product was dissolved into 1,4-dioxane (8 mL), and a 1,4-dioxane solution (4 M) of HCl (4 mL, 16 mmol) was added. The mixture was stirred at room temperature for 1 h and then concentrated. The residue was triturated in diethyl ether, and the precipitate was collected, washed with diethyl ether, and dried *in vacuo* to give the title compound as a HCl salt: a white solid (4.4 g, 86%). LCMS (API): mass calcd. for $C_{23}H_{22}ClN_5O_2S{\cdot}HCl$, 467.1; *m/z* found, 468.1 $[M + H]^+$; ^1H NMR (300 MHz, DMSO-d_6) δ 9.03 (br s, 2H), 8.89 (d, J = 1.9 Hz, 1H), 8.53 (d, J = 2.0 Hz, 1H), 7.33 (d, J = 8.6 Hz, 2H), 7.21 (d, J = 8.5 Hz, 2H), 4.63−4.84 (m, 1H), 3.20−3.29 (m, 2H), 3.02−3.17 (m, 2H), 2.54−2.67 (m, 2H), 2.34−2.46 (m, 2H), 2.09−2.25 (m, 2H), 1.82−2.05 (m, 3H), 1.45−1.63 (m, 1H) ppm.

Preparation of 5-(5-(6-((1-methylpiperidin-4-yl)oxy)pyridin-3-yl)-8-oxo-6-thioxo-5,7-diazaspiro[3.4]octan-7-yl)-3-(trifluoromethyl)picolinonitrile (7). To a mixture of 5-(8-oxo-5-(6-(piperidin-4-yloxy)pyridin-3-yl)-6-thioxo-5,7-diazaspiro[3.4]octan-7-yl)-3-(trifluoromethyl)picolinonitrile TFA salt, **5** (17 g, 27.8 mmol) in THF (150 mL) was added an aqueous solution (37%) of formaldehyde (4.2 mL, 55.6 mmol), followed by the addition of sodium triacetoxyborohydride (9.3 g, 41.7 mmol). The reaction mixture was stirred at room temperature for overnight. The mixture was partitioned between ethyl acetate and aqueous Na_2CO_3 solution (1 M). The organic layer was separated, and the aqueous layer was extracted with ethyl acetate. The combined organic extract was concentrated. The crude residue was purified by chromatography (SiO_2, 0−10% MeOH in DCM) to give the crude product, which was triturated in diethyl ether to give pure salt free product (16.19 g). The product was dissolved into 1,4-dioxane (150 mL), and a 1,4-dioxane solution (4 M) of HCl (8.6 mL, 34 mmol) was added. The mixture was stirred at room temperature for 1 h and then concentrated. The residue was triturated in diethyl ether, and the precipitate was collected, washed with diethyl ether, and dried *in vacuo* to give the title compound as a HCl salt: a white solid (13.6 g, 89%). LCMS (API): mass calcd. for $C_{24}H_{23}F_3N_6O_2S{\cdot}HCl$, 516.2; *m/z* found, 517.1 $[M + H]^+$; ^1H NMR (300 MHz, DMSO-d_6) δ 10.72 (s, 1H), 9.22 (d, J = 2.1 Hz, 1H), 8.75 (d, J = 2.1 Hz, 1H), 8.23 (d, J = 2.6 Hz, 1H), 7.81 (dd, J = 8.7, 2.6 Hz, 1H), 7.08 (d, J = 8.8 Hz, 1H), 5.10−5.51 (m, 1H), 3.32−3.54 (m, 2H), 3.04−3.26 (m, 2H), 2.77 (br s, 3H), 2.57−2.71 (m, 2H), 2.37−2.51 (m, 2H), 1.87−2.36 (m, 5H), 1.50−1.70 (m, 1H) ppm; Anal. Calcd for $C_{24}H_{23}F_3N_6O_2S{\cdot}HCl{\cdot}H_2O$: C, 50.48; H, 4.59; N, 14.72; Found: C, 51.31; H, 4.45; N, 14.46.

Preparation of 5-(8-oxo-5-(2-(piperidin-4-yloxy)pyrimidin-5-yl)-6-thioxo-5,7-diazaspiro[3.4]octan-7-yl)-3-(trifluoromethyl)picolinonitrile (10). Step A. To a solution of *tert*-butyl 4-((5-aminopyrimidin-2-yl)oxy)piperidine-1-carboxylate (**18c**) (Matrix, 2.71 g, 9.23 mmol) in acetic acid (45 mL) was added cyclobutanone (1.38 mL, 18.5 mmol), followed by the addition of sodium cyanide (0.90 g, 18.5 mmol). The reaction mixture was stirred at room temperature for overnight. The mixture was then concentrated under reduced pressure in a fume hood. The residue was taken up in ethyl acetate (50 mL) and washed with 1 M Na_2CO_3 (100 mL) and brine (25 mL) successively. The organic layer was separated, dried over $MgSO_4$, filtered, and concentrated. The crude oily residue was purified by chromatography (SiO_2, 1−60% EA in heptane) to give *tert*-butyl 4-((5-((1-cyanocyclobutyl)amino)-pyrimidin-2-yl)oxy)piperidine-1-carboxylate (**19c**) as a colorless oil (2.47 g, 71%). MS: mass calcd. for $C_{19}H_{27}N_5O_3$, 373.2; *m/z* found, 318.0 $[M + H\text{-}tBu]^+$; ^1H NMR (300 MHz, $CDCl_3$) δ 8.05 (s, 2H), 5.00−5.16 (m, 1H), 3.70−3.91 (m, 3H), 3.17−3.37 (m, 2H), 2.68−2.88 (m, 2H), 2.31−2.45 (m, 2H), 2.12−2.31 (m, 2H), 1.91−2.07 (m, 2H), 1.72−1.86 (m, 2H), 1.47 (s, 9H) ppm.

Step B. To a solution of *tert*-butyl 4-((5-((1-cyanocyclobutyl)-amino)pyrimidin-2-yl)oxy)piperidine-1-carboxylate (**19c**) (2.47 g, 6.61 mmol) in DMA (35 mL) was added freshly prepared 5-isothiocyanato-3-trifluoromethyl-pyridine-2-carbonitrile (**21a**) (2.73 g, 11.9 mmol). The reaction mixture was heated at 60 °C for 4 h. The mixture was cooled to room temperature, and MeOH (7 mL) and HCl (1 M, 7 mL) were added. The mixture was stirred at room temperature for overnight. Ethyl acetate (50 mL) was added, and the mixture washed with water (100 mL), aqueous saturated Na_2CO_3 (1M, 30 mL), and brine (50 mL) successively. The organic layer was separated, dried over $MgSO_4$, filtered, and concentrated. The residue was purified by chromatography (SiO_2, 0−50% EtOAc in heptane) to yield *tert*-butyl 4-((5-(7-(6-cyano-5-(trifluoromethyl)pyridin-3-yl)-8-oxo-6-thioxo-5,7-diazaspiro[3.4]octan-5-yl)pyrimidin-2-yl)oxy)-piperidine-1-carboxylate (**22f**) as an amorphous solid (3.40 g, 85%). MS: mass calcd. for $C_{27}H_{28}F_3N_7O_4S$, 603.2; *m/z* found, 547.9 $[M+H\text{-}tBu]^+$; ^1H NMR (300 MHz, $CDCl_3$) δ 9.08 (d, J = 2.2 Hz, 1H), 8.50 (s, 2H), 8.34 (d, J = 2.2 Hz, 1H), 5.21−5.40 (m, 1H), 3.76−3.96 (m, 2H), 3.25−3.44 (m, 2H), 2.69−2.87 (m, 2H), 2.42−2.60 (m, 2H), 2.23−2.40 (m, 1H), 2.00−2.18 (m, 2H), 1.73−1.98 (m, 3H), 1.48 (s, 9H) ppm.

Step C. To a solution of *tert*-butyl 4-((5-(7-(6-cyano-5-(trifluoromethyl)pyridin-3-yl)-8-oxo-6-thioxo-5,7-diazaspiro[3.4]-octan-5-yl)pyrimidin-2-yl)oxy)piperidine-1-carboxylate (**22f**) (3.40 g, 5.63 mmol) in dioxane (25 mL) was added an anhydrous 1,4-dioxane solution (4 N) of HCl (14.0 mL, 56.0 mmol). The reaction mixture was stirred at room temperature for overnight. The mixture was diluted with diethyl ether (150 mL) and triturated for 2 h. The precipitate was collected by filtration and dried *in vacuo* to give the title compound as a HCl salt: a white solid (2.86 g, 94%). MS: mass calcd. for $C_{22}H_{20}F_3N_7O_2S{\cdot}HCl$, 503.2; *m/z* found, 504.0 $[M + H]^+$; ^1H NMR (300 MHz, DMSO-d_6) δ 9.21 (d, J = 2.0 Hz, 1H), 9.08 (br s, 2H), 8.75 (d, J = 2.0 Hz, 1H), 8.74 (s, 2H), 5.17-5.47 (m, 1H), 3.21-3.35 (m, 2H), 3.05-3.21 (m, 2H), 2.58-2.73 (m, 2H), 2.42-2.59 (m, 2H), 2.17-2.32 (m, 2H), 1.92-2.11 (m, 3H), 1.52-1.75 (m, 1H) ppm.

Preparation of 5-(5-(2-((1-methylpiperidin-4-yl)oxy)-pyrimidin-5-yl)-8-oxo-6-thioxo-5,7-diazaspiro[3.4]octan-7-yl)-3-(trifluoromethyl)picolinonitrile (9). Step A. To a solution of 5-(8-oxo-5-(2-(piperidin-4-yloxy)pyrimidin-5-yl)-6-thioxo-5,7-diazaspiro[3.4]octan-7-yl)-3-(trifluoromethyl)picolinonitrile, **10** (2.88 g, 5.31 mmol) and sodium acetate (0.436 g, 5.31 mmol) in DCE (15 mL) was added formaldehyde (37 wt % in water, 2.8 mL, 37.2 mmol). The mixture was stirred at room temperature for 40 min, and then sodium triacetoxyborohydride (1.78 g, 7.96 mmol) was added in three portions during a period of 45 min. The reaction mixture was stirred for 2 h and then diluted with DCM (125 mL). The mixture was washed successively with aqueous Na_2CO_3 (1 M, 100 mL) and water (50 mL). The organic layer was separated, dried over $MgSO_4$, filtered, and concentrated. The residue was purified by chromatography (SiO_2, 0−15% MeOH in DCM to give the title compound as a white foam (2.27 g, 82%). MS: mass calcd. for $C_{23}H_{22}F_3N_7O_2S$, 517.2; *m/z* found, 518.1 $[M + H]^+$; ^1H NMR (300 MHz, $CDCl_3$) δ 9.09 (d, J = 2.2 Hz, 1H), 8.50 (s, 2H), 8.35 (d, J = 2.2 Hz, 1H), 5.00-5.27 (m, 1H), 2.69-2.94 (m, 4H), 2.42-2.59 (m, 2H), 2.35 (s, 3H), 2.25-2.42

https://dx.doi.org/10.1021/acs.jmedchem.0c01563
J. Med. Chem. 2021, 64, 909−924

(m, 3H), 2.09-2.23 (m, 2H), 1.94-2.09 (m, 2H), 1.69-1.90 (m, 1H) ppm.

Step B. To the solution of 5-(5-(2-((1-methylpiperidin-4-yl)oxy)-pyrimidin-5-yl)-8-oxo-6-thioxo-5,7-diazaspiro[3.4]octan-7-yl)-3-(trifluoromethyl)picolinonitrile, **9** (2.27 g, 4.38 mmol) in 1,4-dioxane (15 mL) was added a 1,4-dioxane solution (4 N) of HCl (1.26 mL, 5.04 mmol). The mixture was stirred at room temperature for 1.5 h, and then diethyl ether (50 mL) was added. The resulting suspension was stirred for another 30 min. The precipitate was collected by filtration through a sintered funnel, washed with diethyl ether (2 × 15 mL), and dried under *in vacuo* to yield the title compound as a HCl salt: a white solid (2.24 g, 89%). MS: mass calcd. for $C_{23}H_{22}F_3N_7O_2S$·HCl, 517.2; *m/z* found, 518.1 $[M + H]^+$; ^1H NMR (300 MHz, DMSO-d_6) δ 10.76 (br s, 1H), 9.22 (s, 1H), 8.75 (s, 3H), 5.38 (br s, 1H), 3.45−3.58 (m, 1H), 3.31−3.43 (m, 2H), 3.08−3.29 (m, 2H), 2.79 (br dd, *J* = 3.30, 13.75 Hz, 3H), 2.60−2.72 (m, 2H), 2.43−2.58 (m, 1H), 2.36 (br d, *J* = 12.65 Hz, 1H), 2.23 (br s, 2H), 1.87−2.15 (m, 2H), 1.54−1.73 (m, 1H) ppm.

Preparation of 5-(8-oxo-5-(4-(piperazin-1-ylmethyl)-phenyl)-6-thioxo-5,7-diazaspiro[3.4]octan-7-yl)-3-(trifluoromethyl)picolinonitrile (16). Step A. Step A. To a solution of *tert*-butyl 4-(4-aminobenzyl)piperazine-1-carboxylate (18d) (Combi-Blocks, 8.53 g, 29.3 mmol) in acetic acid (120 mL) was added cyclobutanone (4.4 mL, 58.5 mmol), followed by the addition of sodium cyanide (2.96 g, 58.5 mmol). The reaction mixture was stirred at room temperature for 3 h. The mixture was then concentrated under reduced pressure in a fume hood. The residue was taken up in ethyl acetate (200 mL) and washed with 1 M Na_2CO_3 (150 mL) and brine (100 mL) successively. The organic layer was separated, dried over $MgSO_4$, filtered, and concentrated. The crude oily residue was purified by chromatography (SiO_2, 10−100% EA in heptane) to give *tert*-butyl 4-(4-((1-cyanocyclobutyl)amino)benzyl)-piperazine-1-carboxylate (19d) as a colorless oil (8.1 g, 67%). MS: mass calcd. for $C_{21}H_{30}N_4O_2$, 370.2; *m/z* found, 371.2 $[M + H]^+$; ^1H NMR (400 MHz, $CDCl_3$) δ 7.17 (d, *J* = 8.28 Hz, 2H), 6.60 (d, *J* = 8.53 Hz, 2H), 4.03 (s, 1H), 3.37−3.45 (m, 6H), 2.75−2.86 (m, 2H), 2.32−2.42 (m, 6H), 2.11−2.30 (m, 2H), 1.45 (s, 9H) ppm.

Step B. To a solution of *tert*-butyl 4-(4-((1-cyanocyclobutyl)-amino)benzyl)piperazine-1-carboxylate (**19d**) (8.1 g, 21.9 mmol) in DMA (30 mL) was added freshly prepared 5-isothiocyanato-3-trifluoromethyl-pyridine-2-carbonitrile (**21a**) (7.5 g, 32.9 mmol). The reaction mixture was heated at 70 °C for 1.5 h. The mixture was cooled to room temperature and MeOH (30 mL) and HCl (1 M, 32.9 mL) were added. The mixture was stirred at room temperature for overnight. Ethyl acetate (50 mL) was added, and the mixture washed with water (100 mL), aqueous saturated Na_2CO_3 (1 M, 30 mL), and brine (50 mL) successively. The organic layer was separated, dried over $MgSO_4$, filtered, and concentrated. The residue was purified by chromatography (SiO_2, 10−65% EtOAc in heptane). The product was further purified by reverse phase chromatography [C18, start (39% H_2O-61%MeCN-MeOH)-end (11% H_2O-89% MeCN-MeOH)]-(25 mM NH_4HCO_3)] to yield *tert*-butyl 4-(4-(7-(6-cyano-5-(trifluoromethyl)pyridin-3-yl)-8-oxo-6-thioxo-5,7-diazaspiro[3.4]octan-5-yl)benzyl)piperazine-1-carboxylate (**22g**) as a white foam (8.7 g, 66%). MS: mass calcd. for $C_{29}H_{31}F_3N_6O_3S$, 600.2; *m/z* found, 601.0 $[M + H]^+$; ^1H NMR (300 MHz, $CDCl_3$) δ 9.11 (d, *J* = 2.3 Hz, 1H), 8.37 (d, *J* = 2.3 Hz, 1H), 7.57 (d, *J* = 7.9 Hz, 2H), 7.27 (d, *J* = 7.1 Hz, 2H), 3.61 (s, 2H), 3.38−3.56 (m, 4H), 2.52−2.81 (m, 4H), 2.40−2.51 (m, 4H), 2.16−2.35 (m, 1H), 1.59−1.80 (m, 1H), 1.46 (s, 9H) ppm.

Step C. To a solution of *tert*-butyl 4-(4-(7-(6-cyano-5-(trifluoromethyl)pyridin-3-yl)-8-oxo-6-thioxo-5,7-diazaspiro[3.4]-octan-5-yl)benzyl)piperazine-1-carboxylate (**22g**) (8.7 g, 14.5 mmol) in DCM (70 mL) was added TFA (15 mL). The reaction mixture was stirred at room temperature for 2 h. The mixture concentrated, and the residue was taken in toluene (40 mL) and again concentrated (2 × 40 mL). The crude residue was diluted with DCM and washed with aqueous Na_2CO_3 solution (1 M). The organic layer was separated, and aqueous layer was extracted with DCM. The combined organic extract was dried over $MgSO_4$, filtered, and concentrated. The residue was purified by reverse phase preparative LC start (70% H_2O-30% MeCN-MeOH)-end (27%H_2O-73%MeCN-MeOH)]-[25 mM NH_4HCO_3]). The salt-free desired product (4.1 g) was dissolved in dioxane (8 mL), and an anhydrous 1,4-dioxane solution (4 N) of HCl (2.25 mL, 9 mmol) was added. The mixture was stirred at room temperature for 1 h. The mixture was diluted with diethyl ether and triturated for overnight. The precipitate was collected by filtration and dried *in vacuo* to give the title compound as a HCl salt: a white solid (4.2 g, 52%). MS: mass calcd. for $C_{24}H_{23}F_3N_6OS$·HCl, 500.2; *m/z* found, 500.9 $[M + H]^+$; ^1H NMR (300 MHz, DMSO-d_6) δ 9.24 (s, 1H), 8.95 (br s, 1H), 8.78 (d, *J* = 1.10 Hz, 1H), 7.58 (br d, *J* = 7.70 Hz, 2H), 7.41 (br d, *J* = 8.25 Hz, 2H), 3.91−4.26 (m, 1H), 3.68 (br s, 2H), 3.58 (s, 1H), 3.26−3.45 (m, 3H), 3.02−3.21 (m, 4H), 2.66 (br s, 2H), 2.45 (br d, *J* = 10.45 Hz, 2H), 1.84−2.14 (m, 1H), 1.43−1.66 (m, 1H) ppm.

Identification of *In Vitro* and *In Vivo* Metabolites. The *in vitro* metabolism was conducted by incubation of 10 μM **4** (JNJ-pan-AR) in 24-well HepatoPac, containing rat, dog, and human hepatocytes cocultured with stroma cells, according to the vendor's protocol at 37 °C for 0 and 7 days. The final organic concentration was 0.1%. Each well was sonicated and scraped prior to protein precipitation with 6 vol of ice-cold 1:1 ratio of acetonitrile to isopropyl alcohol containing 0.1% formic acid. The content from each well was mixed and then transferred to test tube. The precipitated proteins were then sonicated and pelleted by centrifugation at 3000*g* for 10 min. The supernatants were transferred to clean test tubes and evaporated to dryness under a gentle stream of nitrogen at room temperature. The residue in each test tube was reconstituted in 300 μL of a 1:2:1 ratio of acetonitrile/water/isopropyl alcohol fortified with 0.1% formic acid, sonicated for 5 min, and the filtrate from centrifugal filtration, using 0.45 μm nylon filter at 20800*g* for 10 min at 8 °C, was used for metabolite profiling by LC-MS.

The *in vivo* metabolism was investigated using plasma samples from 14-day repeat dose investigation of oral toxicity study of **4** (JNJ-pan-AR) at 50 mg/kg/day and 45 mg/kg/day in rats and dogs, respectively. The rat and dog plasma samples were pooled by equal volumes to create pooled samples corresponding to day 0 and 13 samples. The pooled plasma samples were protein precipitated with two volumes of a 1:1 ratio of acetonitrile and isopropyl alcohol containing 0.1% formic acid. The resulting samples were sonicated and centrifuged at 3000 g for 10 min. The supernatants were diluted with equal volume of 0.1% formic acid, and then filtered through 0.45 μm nylon filters by centrifugation at 20800*g* for 10 min at 8 °C prior to analysis by LC-MS.

All LC-MS analysis was conducted on an Accela UHPLC connected to an LTQ Orbitrap XL (Thermo Scientific, Bremen, Germany) operated in positive ionization mode unless indicated. The chromatographic separation was achieved on a Phenyl-Hexyl LC column (150 × 1 mm ID, 5 μm; Thermo Scientific, Bellefonte, Pa) using a nonlinear gradient consisting of 0.2% formic acid (mobile phase A) and acetonitrile containing 0.2% formic acid (mobile phase B). The column was flow at 0.1 mL/min and kept at 45 °C throughout the analysis. All mass spectrometric analysis was carried out using high resolution accurate mass data-dependent multiple-stage mass analysis. The mass resolution was set at 30,000 and 7,500 for full scan and data-dependent multiple stage mass analysis, respectively. The drug and its metabolites were detected using MsCompare (MsMetrix, The Netherlands).

4 (JNJ-pan-AR) was metabolized *in vitro* to 4 metabolites, M1−4. Structure elucidation of metabolites M1, M2, M3, and M4 was based on the chemical formulas of $C_{19}H_{14}F_3N_4O_2S$ (13.5 RDB, 0.006 ppm), $C_{25}H_{25}F_3N_5O_3S$ (14.5 RDB, −0.003 ppm), $C_{25}H_{25}F_3N_5O_3$ (14.5 RDB, −0.001 ppm), and $C_{24}H_{23}F_3N_5O_2S$ (14.5 RDB, 0.006 ppm) determined from the protonated molecules at *m/z* 419.0784, 532.1625, 500.1904 and 502.1519, respectively. Therefore, M1, M2, M3, and M4 was postulated from metabolism of **4** (JNJ-pan-AR) via O-dealkylation, N-oxidation, oxidative desulfuration and N-demethylation, respectively. The individual structure of M1, M2, M3, or M4 metabolite was confirmed using respective synthetic standard. Metabolites M1−M4 were also identified in pooled day 0 and 13

https://dx.doi.org/10.1021/acs.jmedchem.0c01563
J. Med. Chem. 2021, 64, 909−924

plasma samples from repeated dose investigation of oral toxicity of **4** (JNJ-pan-AR) in rats and dogs.

GSH Screen for Phenolic Metabolites of Androgen Receptor Antagonists. The bioactivation of potential phenolic metabolites of androgen receptor antagonists was evaluated by modification of trapping procedure previously reported by Lim et al., 2008. Briefly, incubation of each potential phenolic metabolite was conducted in a final volume 1 mL in a test tune, containing 10 μM test compound, 1 mg/mL dog liver microsomes, 5 mM glutathione mixture (GSH: [$^{13}C_2$, ^{15}N-glycine]GSH 2:1), and 1 mM NADPH in 0.1 M phosphate buffer. The control sample contained all except the NADPH cofactor. The samples were incubated for 60 min. Once the incubations were completed, the reaction was quenched with 5.0 mL of a 1:1 ratio of acetonitrile and isopropyl alcohol containing 0.1% formic acid. The resulting mixture was vortex mixed and sonicated, followed by centrifugation at 3000g for 10 min at 5 °C. The supernatants were transferred into clean tubes and dried under nitrogen at room temperature to dryness. The residue was dissolved in 300 μL of a 4:1 ratio of 0.1% formic acid and acetonitrile, sonicated, and filtered through 0.45 μm Nylon filters prior to LC-MS analysis.

The glutathione conjugate was detected by isotopic pattern triggered data-dependent multiple-stage high resolution accurate mass analysis. The mining for glutathione conjugates was by high resolution accurate mass isotopic pattern filtering (MsMetrix, The Netherlands) of full scan MS data. The product ion mass spectra were used to elucidate the site of bioactivation.

The identification of glutathione conjugate of phenol **6** at 24.2 min was from the correct chemical formula of $C_{29}H_{29}O_9F_3S_2$ (17.5 RDB, 1.76 ppm), which upon collision-induced dissociation (CID) resulted in cleavage of the C−S bond linking the sulfur atom to the carbon atom of the tripeptide to give m/z 465.0316 ($C_{19}H_{12}O_3N_4F_3S_2$, 14.5 RDB, 3.97 ppm). Such bond cleavage is diagnostic of an aryl thioether. Further isolation of m/z 465 for further CID produced the base peak at m/z 208.0422 (6.5 RDB, −1.90 ppm), which localized the site of hydroxylation and addition of glutathione molecule to the phenolic moiety. The identity of the glutathione conjugate is consistent with bioactivation of phenol **6** to an *o*-quinone prior to addition of the glutathione molecule.

All experimental procedures were conducted in accordance with Janssen's Institutional Animal Care and Use Committee and U.S. Department of Agriculture regulations.

■ ASSOCIATED CONTENT

Supporting Information

The Supporting Information is available free of charge at https://pubs.acs.org/doi/10.1021/acs.jmedchem.0c01563.

Homology model coordinates (PDB)
Molecular formula strings and some data (CSV)
Assay and protocols: radioligand binding, transcriptional reporter, high-content imaging, proliferation, Hershberger, tumor xenograft efficacy, chemistry, ^1H NMR/LCMS/HPLC traces of compounds **4**, **5**, **8**, and molecular modeling (PDF)

■ AUTHOR INFORMATION

Corresponding Authors

Zhuming Zhang − *Janssen Research and Development, Spring House, Pennsylvania 19477, United States;* orcid.org/0000-0002-5638-5320; Email: zzhang85@its.jnj.com

Gilles Bignan − *Janssen Research and Development, Spring House, Pennsylvania 19477, United States;* Email: gbignan@its.jnj.com

Authors

Peter J. Connolly − *Janssen Research and Development, Spring House, Pennsylvania 19477, United States*

Heng Keang Lim − *Janssen Research and Development, Spring House, Pennsylvania 19477, United States*

Vineet Pande − *Janssen Research and Development, B-2340 Beerse, Belgium*

Lieven Meerpoel − *Janssen Research and Development, B-2340 Beerse, Belgium*

Christopher Teleha − *Janssen Research and Development, Spring House, Pennsylvania 19477, United States*

Jonathan R. Branch − *Janssen Research and Development, Spring House, Pennsylvania 19477, United States;* orcid.org/0000-0003-4169-5753

Janine Ondrus − *Janssen Research and Development, Spring House, Pennsylvania 19477, United States*

Ian Hickson − *Janssen Research and Development, Spring House, Pennsylvania 19477, United States;* orcid.org/0000-0002-9167-0514

Tammy Bush − *Janssen Research and Development, Spring House, Pennsylvania 19477, United States*

Leopoldo Luistro − *Janssen Research and Development, Spring House, Pennsylvania 19477, United States*

Kathryn Packman − *Janssen Research and Development, Cambridge, Massachusetts 02142, United States*

James R. Bischoff − *Janssen Research and Development, Spring House, Pennsylvania 19477, United States*

Salam Ibrahim − *Janssen Research and Development, Spring House, Pennsylvania 19477, United States*

Christopher Parrett − *VWR Avantor, Spring House, Pennsylvania 19477, United States*

Yolanda Chong − *Janssen Research and Development, B-2340 Beerse, Belgium*

Marco M. Gottardis − *Janssen Research and Development, Spring House, Pennsylvania 19477, United States*

Complete contact information is available at: https://pubs.acs.org/10.1021/acs.jmedchem.0c01563

Author Contributions

The manuscript was written through contributions of all authors. Contributions by C.T., I.H., J.R.B., and Y.C. were performed while employed at Janssen Research and Development.

Notes

The authors declare no competing financial interest.

■ ACKNOWLEDGMENTS

The authors would like to thank Nick Smith and Mark Herbert (Aragon Pharmaceuticals, San Diego, CA) for their valuable insights into early SAR of the thiohydantoin series. We are also grateful to Luis Trabalón Escolar and Christian Rocaboy (Eurofins Villapharma, Spain) and Bing Huang (Wuxi AppTec, Shanghai, China) for their contributions to synthesis of compounds described herein.

■ ABBREVIATIONS

AR, androgen receptor; ADT, androgen deprivation therapy; CRPC, castration resistant prostate cancer; LBD, ligand binding domain; GSH, glutathione; NADPH, nicotinamide adenine dinucleotide phosphate hydrogen; MFS, metastasis-free survival; NTD, N-terminal domain; DBD, DNA-binding domain; AF1, activation function 1; AF2, activation function 2; ctDNA, circulating tumor DNA; GR, glucocorticoid receptor; ER, estrogen receptor; PSA, prostate-specific antigen; ARE, androgen response element; KLK3, kallikrein-3, also known as

PSA; ASO, androgen sensitive organ; TP, testosterone propionate; TGI, tumor growth inhibition; ALP, alkaline phosphatase; ALT, alanine aminotransferase; GGT, gamma-glutamyl transferase; PD, pharmacodynamics; PK, pharmacokinetics; HLM, human liver microsomes; ESI, electrospray ionization; API, atmospheric pressure chemical ionization; DMA, dimethylacetamide; EtOAc, ethyl acetate

REFERENCES

(1) Fujita, K.; Nonomura, N. Role of androgen receptor in prostate cancer: a review. *World J. Mens Health.* **2019**, *37* (3), 288−295.

(2) De Bono, J. S.; Logothetis, C. J.; Molina, A.; Fizazi, K.; North, S.; Chu, L.; Chi, K. N.; Jones, R. J.; Goodman, O. B., Jr; Saad, F.; Staffurth, J. N.; Mainwaring, P.; Harland, S.; Flaig, T. W.; Hutson, T. E.; Cheng, T.; Patterson, H.; Hainsworth, J. D.; Ryan, C. J.; Sternberg, C. N.; Ellard, S. L.; Fléchon, A.; Saleh, M.; Scholz, M.; Efstathiou, E.; Zivi, A.; Bianchini, D.; Loriot, Y.; Chieffo, N.; Kheoh, T.; Haqq, C. M.; Scher, H. I. Abiraterone and increased survival in metastatic prostate cancer. *N. Engl. J. Med.* **2011**, *364* (21), 1995−2005.

(3) Scher, H. I.; Fizazi, K.; Saad, F.; Taplin, M. E.; Sternberg, C. N.; Miller, K.; de Wit, R.; Mulders, P.; Chi, K. N.; Shore, N. D.; Armstrong, A. J.; Flaig, T. W.; Fléchon, A.; Mainwaring, P.; Fleming, M.; Hainsworth, J. D.; Hirmand, M.; Selby, B.; Seely, L.; de Bono, J. S. Increased survival with enzalutamide in prostate cancer after chemotherapy. *N. Engl. J. Med.* **2012**, *367* (13), 1187−1197.

(4) Smith, M. R.; Saad, F.; Chowdhury, S.; Oudard, S.; Hadaschik, B. A.; Graff, J. N.; Olmos, D.; Mainwaring, P. N.; Lee, J. Y.; Uemura, H.; Lopez-Gitlitz, A.; Trudel, G. C.; Espina, B. M.; Shu, Y.; Park, Y. C.; Rackoff, W. R.; Yu, M. K.; Small, E. J. Apalutamide treatment and metastasis-free survival in prostate cancer. *N. Engl. J. Med.* **2018**, *378* (15), 1408−1418.

(5) Hussain, M.; Fizazi, K.; Saad, F.; Rathenborg, P.; Shore, N.; Ferreira, U.; Ivashchenko, P.; Demirhan, E.; Modelska, K.; Phung, D.; Krivoshik, A.; Sternberg, C. N. Enzalutamide in men with non-metastatic, castration-resistant prostate cancer. *N. Engl. J. Med.* **2018**, *378* (26), 2465−2474.

(6) Crona, D. J.; Milowsky, M. I.; Whang, Y. E. Androgen receptor targeting drugs in castration-resistant prostate cancer and mechanisms of resistance. *Clin. Pharmacol. Ther.* **2015**, *98* (6), 582−589.

(7) Quigley, D. A.; Dang, H. X.; Zhao, S. G.; Lloyd, P.; Aggarwal, R.; Alumkal, J. J.; Foye, A.; Kothari, V.; Perry, M. D.; Bailey, A. M.; Playdle, D.; Barnard, T. J.; Zhang, L.; Zhang, J.; Youngren, J. F.; Cieslik, M. P.; Parolia, A.; Beer, T. M.; Thomas, G.; Chi, K. N.; Gleave, M.; Lack, N. A.; Zoubeidi, A.; Reiter, R. E.; Rettig, M. B.; Witte, O.; Ryan, C. J.; Fong, L.; Kim, W.; Friedlander, T.; Chou, J.; Li, H.; Das, R.; Li, H.; Moussavi-Baygi, R.; Goodarzi, H.; Gilbert, L. A.; Lara, P. N., Jr; Evans, C. P.; Goldstein, T. C.; Stuart, J. M.; Tomlins, S. A.; Spratt, D. E.; Cheetham, R. K.; Cheng, D. T.; Farh, K.; Gehring, J. S.; Hakenberg, J.; Liao, A.; Febbo, P. G.; Shon, J.; Sickler, B.; Batzoglou, S.; Knudsen, K. E.; He, H. H.; Huang, J.; Wyatt, A. W.; Dehm, S. M.; Ashworth, A.; Chinnaiyan, A. M.; Maher, C. A.; Small, E. J.; Feng, F. Y. Genomic hallmarks and structural variation in metastatic prostate cancer. *Cell* **2018**, *174* (3), 758−769.

(8) Robinson, D.; Van Allen, E. M.; Wu, Y. M.; Schultz, N.; Lonigro, R. J.; Mosquera, J. M.; Montgomery, B.; Taplin, M. E.; Pritchard, C. C.; Attard, G.; Beltran, H.; Abida, W.; Bradley, R. K.; Vinson, J.; Cao, X.; Vats, P.; Kunju, L. P.; Hussain, M.; Feng, F. Y.; Tomlins, S. A.; Cooney, K. A.; Smith, D. C.; Brennan, C.; Siddiqui, J.; Mehra, R.; Chen, Y.; Rathkopf, D. E.; Morris, M. J.; Solomon, S. B.; Durack, J. C.; Reuter, V. E.; Gopalan, A.; Gao, J.; Loda, M.; Lis, R. T.; Bowden, M.; Balk, S. P.; Gaviola, G.; Sougnez, C.; Gupta, M.; Yu, E. Y.; Mostaghel, E. A.; Cheng, H. H.; Mulcahy, H.; True, L. D.; Plymate, S. R.; Dvinge, H.; Ferraldeschi, R.; Flohr, P.; Miranda, S.; Zafeiriou, Z.; Tunariu, N.; Mateo, J.; Perez-Lopez, R.; Demichelis, F.; Robinson, B. D.; Schiffman, M.; Nanus, D. M.; Tagawa, S. T.; Sigaras, A.; Eng, K. W.; Elemento, O.; Sboner, A.; Heath, E. I.; Scher, H. I.; Pienta, K. J.; Kantoff, P.; de Bono, J. S.; Rubin, M. A.; Nelson, P. S.; Garraway, L. A.; Sawyers, C. L.; Chinnaiyan, A. M. Integrative clinical genomics of advanced prostate cancer. *Cell* **2015**, *161* (5), 1215−1228.

(9) Antonarakis, E. S.; Lu, C.; Wang, H.; Luber, B.; Nakazawa, M.; Roeser, J. C.; Chen, Y.; Mohammad, T. A.; Chen, Y.; Fedor, H. L.; Lotan, T. L.; Zheng, Q.; De Marzo, A. M.; Isaacs, J. T.; Isaacs, W. B.; Nadal, R.; Paller, C. J.; Denmeade, S. R.; Carducci, M. A.; Eisenberger, M. A.; Luo, J. AR-V7 and resistance to enzalutamide and abiraterone in prostate cancer. *N. Engl. J. Med.* **2014**, *371* (11), 1028−1038.

(10) Joseph, J. D.; Lu, N.; Qian, J.; Sensintaffar, J.; Shao, G.; Brigham, D.; Moon, M.; Maneval, E. C.; Chen, I.; Darimont, B.; Hager, J. H. A clinically relevant androgen receptor mutation confers resistance to second-generation antiandrogens enzalutamide and ARN-509. *Cancer Discovery* **2013**, *3* (9), 1020−1029.

(11) Korpal, M.; Korn, J. M.; Gao, X.; Rakiec, D. P.; Ruddy, D. A.; Doshi, S.; Yuan, J.; Kovats, S. G.; Kim, S.; Cooke, V. G.; Monahan, J. E.; Stegmeier, F.; Roberts, T. M.; Sellers, W. R.; Zhou, W.; Zhu, P. An F876L mutation in androgen receptor confers genetic and phenotypic resistance to MDV3100 (enzalutamide). *Cancer Discovery* **2013**, *3* (9), 1030−1043.

(12) Arora, V. K.; Schenkein, E.; Murali, R.; Subudhi, S. K.; Wongvipat, J.; Balbas, M. D.; Shah, N.; Cai, L.; Efstathiou, E.; Logothetis, C.; Zheng, D.; Sawyers, C. L. Glucocorticoid receptor confers resistance to antiandrogens by bypassing androgen receptor blockade. *Cell* **2013**, *155* (6), 1309−1322.

(13) Azad, A. A.; Volik, S. V.; Wyatt, A. W.; Haegert, A.; Le Bihan, S.; Bell, R. H.; Anderson, S. A.; McConeghy, B.; Shukin, R.; Bazov, J.; Youngren, J.; Paris, P.; Thomas, G.; Small, E. J.; Wang, Y.; Gleave, M. E.; Collins, C. C.; Chi, K. N. Androgen receptor gene aberrations in circulating cell-free DNA: biomarkers of therapeutic resistance in castration-resistant prostate cancer. *Clin. Cancer Res.* **2015**, *21* (10), 2315−2324.

(14) Li, Y.; Chan, S. C.; Brand, L. J.; Hwang, T. H.; Silverstein, K. A.; Dehm, S. M. Androgen receptor splice variants mediate enzalutamide resistance in castration-resistant prostate cancer cell lines. *Cancer Res.* **2013**, *73* (2), 483−489.

(15) Hait, W. N.; Lebowitz, P. F. Moving upstream in anticancer drug development. *Nat. Rev. Drug Discovery* **2019**, *18* (3), 159−160.

(16) Tan, M. H.; Li, J.; Xu, H. E.; Melcher, K.; Yong, E. L. Androgen receptor: structure, role in prostate cancer and drug discovery. *Acta Pharmacol. Sin.* **2015**, *36* (1), 3−23.

(17) Rathkopf, D. E.; Smith, M. R.; Ryan, C. J.; Berry, W. R.; Shore, N. D.; Liu, G.; Higano, C. S.; Alumkal, J. J.; Hauke, R.; Tutrone, R. F.; Saleh, M.; Chow Maneval, E.; Thomas, S.; Ricci, D. S.; Yu, M. K.; de Boer, C. J.; Trinh, A.; Kheoh, T.; Bandekar, R.; Scher, H. I.; Antonarakis, E. S. Androgen receptor mutations in patients with castration-resistant prostate cancer treated with apalutamide. *Ann. Oncol.* **2017**, *28* (9), 2264−2271.

(18) van de Wijngaart, D. J.; Molier, M.; Lusher, S. J.; Hersmus, R.; Jenster, G.; Trapman, J.; Dubbink, H. J. Systematic structure-function analysis of androgen receptor Leu701 mutants explains the properties of the prostate cancer mutant L701H. *J. Biol. Chem.* **2010**, *285* (7), 5097−5105.

(19) Tan, J.; Sharief, Y.; Hamil, K. G.; Gregory, C. W.; Zang, D. Y.; Sar, M.; Gumerlock, P. H.; deVere White, R. W.; Pretlow, T. G.; Harris, S. E.; Wilson, E. M.; Mohler, J. L.; French, F. S. Dehydroepiandrosterone activates mutant androgen receptors expressed in the androgen-dependent human prostate cancer xenograft CWR22 and LNCaP cells. *Mol. Endocrinol.* **1997**, *11* (4), 450−459.

(20) Hara, T.; Miyazaki, J.; Araki, H.; Yamaoka, M.; Kanzaki, N.; Kusaka, M.; Miyamoto, M. Novel mutations of androgen receptor: a possible mechanism of bicalutamide withdrawal syndrome. *Cancer Res.* **2003**, *63* (1), 149−153.

(21) Taplin, M. E.; Bubley, G. J.; Ko, Y. J.; Small, E. J.; Upton, M.; Rajeshkumar, B.; Balk, S. P. Selection for androgen receptor mutations in prostate cancers treated with androgen antagonist. *Cancer Res.* **1999**, *59* (11), 2511−2515.

(22) Moilanen, A. M.; Riikonen, R.; Oksala, R.; Ravanti, L.; Aho, E.; Wohlfahrt, G.; Nykänen, P. S.; Törmäkangas, O. P.; Palvimo, J. J.;

https://dx.doi.org/10.1021/acs.jmedchem.0c01563
J. Med. Chem. 2021, 64, 909−924

Kallio, P. J. Discovery of ODM-201, a new-generation androgen receptor inhibitor targeting resistance mechanisms to androgen signaling-directed prostate cancer therapies. *Sci. Rep.* **2015**, *5*, 12007.
(23) Smith, N. D.; Bonnefous, C.; Julien, J. D. Androgen Receptor Modulator and Uses thereof. *PCT Int. Appl.* Aug 25, 2011, WO 2011103202 A2.
(24) Hsieh, C. L.; Cai, C.; Giwa, A.; Bivins, A.; Chen, S. Y.; Sabry, D.; Govardhan, K.; Shemshedini, L. Expression of a hyperactive androgen receptor leads to androgen-independent growth of prostate cancer cells. *J. Mol. Endocrinol.* **2008**, *41* (1), 13−23.
(25) Clegg, N. J.; Wongvipat, J.; Joseph, J. D.; Tran, C.; Ouk, S.; Dilhas, A.; Chen, Y.; Grillot, K.; Bischoff, E. D.; Cai, L.; Aparicio, A.; Dorow, S.; Arora, V.; Shao, G.; Qian, J.; Zhao, H.; Yang, G.; Cao, C.; Sensintaffar, J.; Wasielewska, T.; Herbert, M. R.; Bonnefous, C.; Darimont, B.; Scher, H. I.; Smith-Jones, P.; Klang, M.; Smith, N. D.; De Stanchina, E.; Wu, N.; Ouerfelli, O.; Rix, P. J.; Heyman, R. A.; Jung, M. E.; Sawyers, C. L.; Hager, J. H. ARN-509: a novel antiandrogen for prostate cancer treatment. *Cancer Res.* **2012**, *72* (6), 1494−1503.
(26) Chen, C. D.; Welsbie, D. S.; Tran, C.; Baek, S. H.; Chen, R.; Vessella, R.; Rosenfeld, M. G.; Sawyers, C. L. Molecular determinants of resistance to antiandrogen therapy. *Nat. Med.* **2004**, *10* (1), 33−39.
(27) van Royen, M. E.; van Cappellen, W. A.; de Vos, C.; Houtsmuller, A. B.; Trapman, J. Stepwise androgen receptor dimerization. *J. Cell Sci.* **2012**, *125* (Pt 8), 1970−1979.
(28) Naven, R. T.; Swiss, R.; Klug-McLeod, J.; Will, Y.; Greene, N. The development of structure-activity relationships for mitochondrial dysfunction: uncoupling of oxidative phosphorylation. *Toxicol. Sci.* **2013**, *131* (1), 271−278.
(29) Kauppi, B.; Jakob, C.; Färnegårdh, M.; Yang, J.; Ahola, H.; Alarcon, M.; Calles, K.; Engström, O.; Harlan, J.; Muchmore, S.; Ramqvist, A. K.; Thorell, S.; Ohman, L.; Greer, J.; Gustafsson, J. A.; Carlstedt-Duke, J.; Carlquist, M. The three-dimensional structures of antagonistic and agonistic forms of the glucocorticoid receptor ligand-binding domain: RU-486 induces a trans conformation that leads to active antagonism. *J. Biol. Chem.* **2003**, *278* (25), 22748−22754.
(30) Liu, H.; Han, R.; Li, J.; Liu, H.; Zheng, L. Molecular mechanism of R-bicalutamide switching from androgen receptor antagonist to agonist induced by amino acid mutations using molecular dynamics simulations and free energy calculation. *J. Comput.-Aided Mol. Des.* **2016**, *30* (12), 1189−1200.
(31) Liu, H. L.; Zhong, H. Y.; Song, T. Q.; Li, J. Z. A molecular modeling study of the hydroxyflutamide resistance mechanism induced by androgen receptor mutations. *Int. J. Mol. Sci.* **2017**, *18* (9), 1823.
(32) Liu, H.; Wang, L.; Tian, J.; Li, J.; Liu, H. Molecular Dynamics Studies on the Enzalutamide resistance mechanisms induced by androgen receptor mutations. *J. Cell. Biochem.* **2017**, *118* (9), 2792−2801.
(33) Nadal, M.; Prekovic, S.; Gallastegui, N.; Helsen, C.; Abella, M.; Zielinska, K.; Gay, M.; Vilaseca, M.; Taulès, M.; Houtsmuller, A. B.; van Royen, M. E.; Claessens, F.; Fuentes-Prior, P.; Estébanez-Perpiñá, E. Structure of the homodimeric androgen receptor ligand-binding domain. *Nat. Commun.* **2017**, *8*, 14388.
(34) Jung, M. E.; Ouk, S.; Yoo, D.; Sawyers, C. L.; Chen, C.; Tran, C.; Wongvipat, J. Structure-activity relationship for thiohydantoin androgen receptor antagonists for castration-resistant prostate cancer (CRPC). *J. Med. Chem.* **2010**, *53* (7), 2779−2796.
(35) Bignan, G.; Connolly, P. J.; Hickson, I.; Meerpoel, L.; Pande, V.; Zhang, Z.; Branch, J.; Rocaboy, C.; Trabalon Escolar, L. B. Preparation of Substituted Thiohydantoin Derivatives as Androgen Receptor Antagonists. *PCT Int. Appl.* Jul 20, 2017, WO 2017123542 A1.
(36) The detailed biological characterization of **5** (JNJ63576253) is being reported in a separate communication.
(37) Lambert, M.; Jambon, S.; Depauw, S.; David-Cordonnier, M. H. Targeting transcription factors for cancer treatment. *Molecules* **2018**, *23* (6), 1479.
(38) Hwang, D. J.; He, Y.; Ponnusamy, S.; Mohler, M. L.; Thiyagarajan, T.; McEwan, I. J.; Narayanan, R.; Miller, D. D. New generation of selective androgen receptor degraders: our initial design, synthesis, and biological evaluation of new compounds with enzalutamide-resistant prostate cancer activity. *J. Med. Chem.* **2019**, *62* (2), 491−511.
(39) ARV-110, a PROTAC compound for targeted AR degradation, is currently being evaluated in a Phase 1 clinical trial (NCT NCT03888612).
(40) Han, X.; Wang, C.; Qin, C.; Xiang, W.; Fernandez-Salas, E.; Yang, C. Y.; Wang, M.; Zhao, L.; Xu, T.; Chinnaswamy, K.; Delproposto, J.; Stuckey, J.; Wang, S. Discovery of ARD-69 as a highly potent proteolysis targeting chimera (PROTAC) degrader of androgen receptor (AR) for the treatment of prostate cancer. *J. Med. Chem.* **2019**, *62* (2), 941−964.
(41) Shibata, N.; Nagai, K.; Morita, Y.; Ujikawa, O.; Ohoka, N.; Hattori, T.; Koyama, R.; Sano, O.; Imaeda, Y.; Nara, H.; Cho, N.; Naito, M. Development of protein degradation inducers of androgen receptor by conjugation of androgen receptor ligands and inhibitor of apoptosis protein ligands. *J. Med. Chem.* **2018**, *61* (2), 543−575.
(42) **5** (JNJ-63576253) is currently being evaluated in a Phase 1/2A clinical trial (NCT02987829).

https://dx.doi.org/10.1021/acs.jmedchem.0c01563
J. Med. Chem. 2021, 64, 909−924